MARINE ECOLOGY

Hypoxia causes preservation of labile organic matter and changes seafloor microbial community composition (Black Sea)

Gerdhard L. Jessen,[1,2]* Anna Lichtschlag,[1,2†] Alban Ramette,[1,2‡] Silvio Pantoja,[3] Pamela E. Rossel,[1,2,4] Carsten J. Schubert,[5] Ulrich Struck,[6] Antje Boetius[1,2]*

Bottom-water oxygen supply is a key factor governing the biogeochemistry and community composition of marine sediments. Whether it also determines carbon burial rates remains controversial. We investigated the effect of varying oxygen concentrations (170 to 0 μM O_2) on microbial remineralization of organic matter in seafloor sediments and on community diversity of the northwestern Crimean shelf break. This study shows that 50% more organic matter is preserved in surface sediments exposed to hypoxia compared to oxic bottom waters. Hypoxic conditions inhibit bioturbation and decreased remineralization rates even within short periods of a few days. These conditions led to the accumulation of threefold more phytodetritus pigments within 40 years compared to the oxic zone. Bacterial community structure also differed between oxic, hypoxic, and anoxic zones. Functional groups relevant in the degradation of particulate organic matter, such as *Flavobacteriia*, *Gammaproteobacteria*, and *Deltaproteobacteria*, changed with decreasing oxygenation, and the microbial community of the hypoxic zone took longer to degrade similar amounts of deposited reactive matter. We conclude that hypoxic bottom-water conditions—even on short time scales—substantially increase the preservation potential of organic matter because of the negative effects on benthic fauna and particle mixing and by favoring anaerobic processes, including sulfurization of matter.

INTRODUCTION

Marine sediments preserve only <1% of the primary produced organic matter because of its efficient remineralization in the water column and on the seafloor by fauna and microorganisms (*1*). Over geological time scales, the burial rate of organic matter affects the global carbon and oxygen cycle; thus, key questions remain as to the environmental factors that alter faunal and microbial transformation of deposited organic matter. One such factor apparently controlling burial and efficiency of organic carbon degradation is bottom-water oxygen concentration (*1*–*4*). Low oxygen supply at the seafloor promotes the accumulation of organic matter in sediments, but the underlying mechanisms for this effect are still not fully elucidated. Previous investigations have compared the effects of oxygen on organic matter degradation rates by assessing oxic versus anoxic conditions or oscillations of both in the field and laboratory (*5*–*10*) and by global data syntheses and modeling [(*3*, *11*) and references therein)]. Because of the increasing spread of hypoxia, it is important to understand and to quantify the consequences of low oxygen supply for marine life, ecosystem function, and biogeochemical cycles (*12*). Hypoxic conditions are defined as oxygen concentrations (<63 μM O_2) known to affect faunal physiology, community structure, and ecosystem function (*10*).

The inhibition of faunal activity has been proposed as a key factor in hypoxia-induced organic matter accumulation (*10*). By dwelling in surface sediments, benthic fauna can actively mix oxygen and fresh organic deposits with deeper anoxic sediment layers, a process termed bioturbation (*1*, *7*, *13*). However, at low bottom-water oxygen concentrations, benthic fauna will emigrate or die, with the consequence that microbes dominate organic matter transformation and benthic energy fluxes in hypoxic environments (*14*). Because microbes do not perturb the sediment, bacterial depolymerization of complex molecules is relatively slow and inefficient in the absence of benthic fauna (*9*, *15*–*17*). Furthermore, although microbial extracellular enzymatic degradation of organic matter does not require oxygen per se, some molecules with nonhydrolyzable bonds can only be cleaved through highly reactive peroxide groups (that is, oxygen–oxygen single bond) or by oxygenases and peroxidases, therefore requiring oxygen as an enzymatic cofactor [(*1*, *3*) and references therein]. Additionally, the accumulation of degradation products, such as sulfide, can change organic matter availability and reactivity, affecting remineralization rates (*18*) and enhancing preservation of otherwise labile compounds over time scales of millennia (*19*). Under oxic conditions, many organisms can fully mineralize the hydrolytic products to carbon dioxide, but in the absence of oxygen, complete organic matter breakdown needs complex consortia of anaerobes [(*4*) and references therein].

Microbial communities inhabiting surface seafloor sediments can rapidly react to input of fresh organic matter: (i) at a functional level, by increasing hydrolysis, respiration, and carbon assimilation rates (*20*, *21*), and (ii) at a community level, by changing their species composition (*22*, *23*). Eutrophic coastal areas and oxygen minimum zones contain highly diverse communities within the top few centimeters of surface sediments, including aerobic and anaerobic polymer degraders, which use a variety of electron acceptors such as nitrate, iron, manganese, and sulfate (*24*–*27*). Shelf sediments receive a relatively high but variable input of organic matter and are generally well mixed by physical and biological processes and exposed to varying fluxes of oxic bottom waters and anoxic pore waters (*28*). Hence, it appears likely that benthic microbial communities are well adapted to fluctuating oxygen availability. However, so far, little is known about the direct effects of hypoxia on communities

[1]Max Planck Institute for Marine Microbiology, Bremen, Germany. [2]HGF MPG Joint Research Group for Deep-Sea Ecology and Technology, Alfred Wegener Institute, Helmholtz Centre for Polar and Marine Sciences, Bremerhaven, Germany. [3]Department of Oceanography and COPAS Sur-Austral, University of Concepción, Concepción, Chile. [4]Research Group for Marine Geochemistry (ICBM-MPI Bridging Group), Institute for Chemistry and Biology of the Marine Environment (ICBM), University of Oldenburg, Oldenburg, Germany. [5]Department of Surface Waters–Research and Management, Swiss Federal Institute of Aquatic Science and Technology, Kastanienbaum, Switzerland. [6]Museum für Naturkunde, Leibniz-Institut für Evolutions- und Biodiversitätsforschung, Berlin, Germany.
*Corresponding author. Email: gjessen@mpi-bremen.de (G.L.J.); antje.boetius@awi.de (A.B.)
†Present address: National Oceanography Centre, Southampton, U.K.
‡Present address: Institute for Infectious Diseases, University of Bern, Bern, Switzerland.

of benthic microorganisms in marine sediments and the impact of temporal variability in oxygen availability. It remains to be tested whether the composition of microorganisms is sensitive to bottom-water oxygen concentration, as is the composition and diversity of benthic fauna (*10*) and at what threshold of oxygen concentration. In the case of the Black Sea, the presence or absence of oxygen (or hydrogen sulfide) has been proposed as the main driver for the changes in microbial community structure and function (*29*–*33*).

The Black Sea is the largest naturally anoxic water body in the world. The permanent stratification of the water column defines an anoxic-sulfidic deepwater mass and a ventilated oxic surface layer separated by a chemocline at a depth of ca. 80 to 100 m (*31*, *34*). The position of the chemocline is dome-shaped, being shallower in the central basin compared to the shelves where it resides at a water depth of about 150 m (*35*). Along the shelf, the chemocline encounters the seafloor, creating a dynamic range of oxygenation regimes within a water depth zone of 100 to 200 m from permanent oxic to variable hypoxic and anoxic-sulfidic conditions (Fig. 1). On the outer northwestern Crimean shelf, internal waves and eddies can oscillate the chemocline across the shelf break, producing drastic changes in bottom-water oxygen availability at the seafloor on a scale of days to hours (*36*).

In this study, we have sampled the northwestern Crimean shelf break (Black Sea) exposed to a natural gradient in bottom-water oxygen concentration within a transect of 40 km. The sites compared are uniform in productivity, particle deposition, and sediment accumulation rate. This sampling design allowed us to assess the direct effect of bottom-water oxygen supply on organic matter preservation, reactivity, faunal and microbial community composition, and the respective threshold for decreased remineralization efficiency for various organic compounds. Sampled sites included, at one extreme, a permanent oxic zone showing oxygen penetration depths of, on average, 5 mm with signs of bioturbation, including oxygen penetration, and roughness, of topography of surface sediments. At the other extreme, the permanent anoxic zone with slightly sulfidic bottom waters lacked fauna, aerobic respiration, and bioturbation. Within the hypoxic zone, we could discriminate two areas of oxic-hypoxic (170 to 10 μM; O_2 penetration depth of 5 to 2 mm) and hypoxic-anoxic conditions (20 to 0 μM; O_2 penetration depth of <2 mm) (Fig. 1). The study focused on the top centimeter of deposited sediment, representing ca. 10 years of sediment accumulation [years 2000–2010; (*37*)]. We tested the hypotheses that variations in oxygen supply cause shifts in structure and function of benthic microbial communities and that this shift leads to the accumulation of labile organic compounds. Specifically, we predicted that (i) we should observe differences in organic matter accumulation along this transect, if there was a link between oxygenation and organic matter remineralization efficiency, and (ii) a change in oxygen concentration would be accompanied by a shift in faunal and microbial community composition, with (iii) effects on the composition of the organic matter buried.

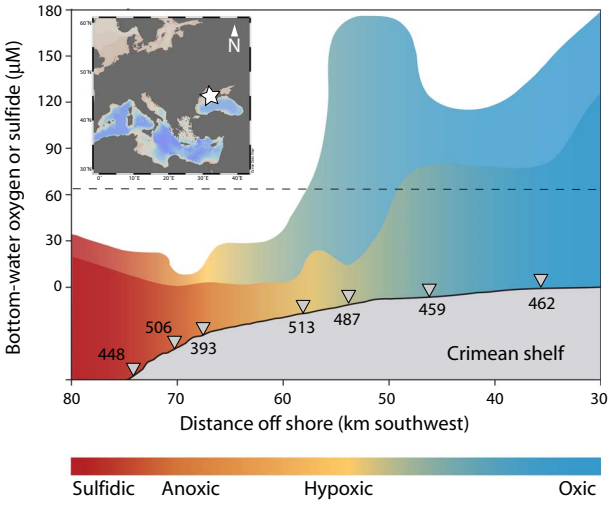

Fig. 1. Study area (inset, star) and section of the outer northwestern Crimean shelf showing the position of sampling sites (inverted triangles). The filled areas show the minimum and maximum bottom-water oxygen or sulfide concentrations measured at different times between 25 April 2010 and 7 May 2010 (n = 128; measured between 0.05 and 12 m above seafloor). Blue, oxic; yellow, hypoxic; red-orange, anoxic-sulfidic conditions. The dashed line depicts the hypoxia threshold (63 μM O_2).

RESULTS

Geochemical gradients related to oxygen content of bottom water

Along a transect of ca. 40 km on the outer Crimean shelf, a continuous decrease in bottom-water oxygen concentration was observed with increasing water depth below 120 m (Fig. 1). Bottom-water oxygen concentration ranged from ca. 170 μM at 100 m to below the detection limit at depths greater than 170 m. Deeper than about 200 m, bottom waters contained 3 to 10 μM sulfide (Fig. 1). Within the hypoxic zone, we could discriminate two areas of oxic-hypoxic (170 to 10 μM; O_2 penetration depth of 5 to 2 mm) and hypoxic-anoxic conditions (20 to 0 μM; O_2 penetration depth of <2 mm) (Fig. 1). Accordingly, four different zones were defined in terms of oxygen supply: (i) permanent oxic, (ii) variable oxic-hypoxic, (iii) variable anoxic-hypoxic, and (iv) permanent anoxic, with sulfide in bottom waters.

A rather constant primary productivity of 220 g C m^{-2} $year^{-1}$, as estimated from ocean color algorithms, prevails for the entire study area [MyOcean data extract (2015); fig. S1] (*38*), of which approximately 30% reaches the seafloor (*38*), equivalent to a particle flux of 15 mmol C m^{-2} day^{-1}. Sediment accumulation rates are around 1 ± 0.5 mm $year^{-1}$ for the upper 10 cm (*37*).

Sediments were of fine-grain muddy composition with a brownish-grayish fluff layer on top (~0.5 cm; Fig. 2). Porosity did not vary considerably along the transect or across the top 10 cm, averaging 0.9 ± 0.03 and 0.8 ± 0.07, respectively (*37*). A change in coloration in surface sediments was observed from beige-brownish in the oxic zone to dark gray in the hypoxic zone and blackish toward anoxic conditions (Fig. 2). The chemocline, as the boundary between oxidized and reduced bottom-water and surficial sediments, was detected visually at a depth of 150 m by the change in faunal traces and sediment color. Oxygen penetration depth measured with microsensors was 5 mm in sediments exposed to permanent oxic conditions, decreasing to <2 mm toward the hypoxic zone and reaching <0.5 mm in the hypoxic-anoxic zone (*37*). Hence, bulk sediment samples analyzed here were mostly anoxic, with the main difference being surface exposure to different bottom-water oxygen concentrations. Only the oxic site showed burrows and other signs of bioturbation and was populated by seafloor-dwelling fauna (Table 1).

Pigments.

Pigment concentrations in surface sediments increased significantly from oxic to anoxic bottom-water conditions ($F_{3,9}$ = 9.39, P < 0.01; Tukey post hoc test, P < 0.05; Fig. 2 and Table 1). Chlorophyll a content

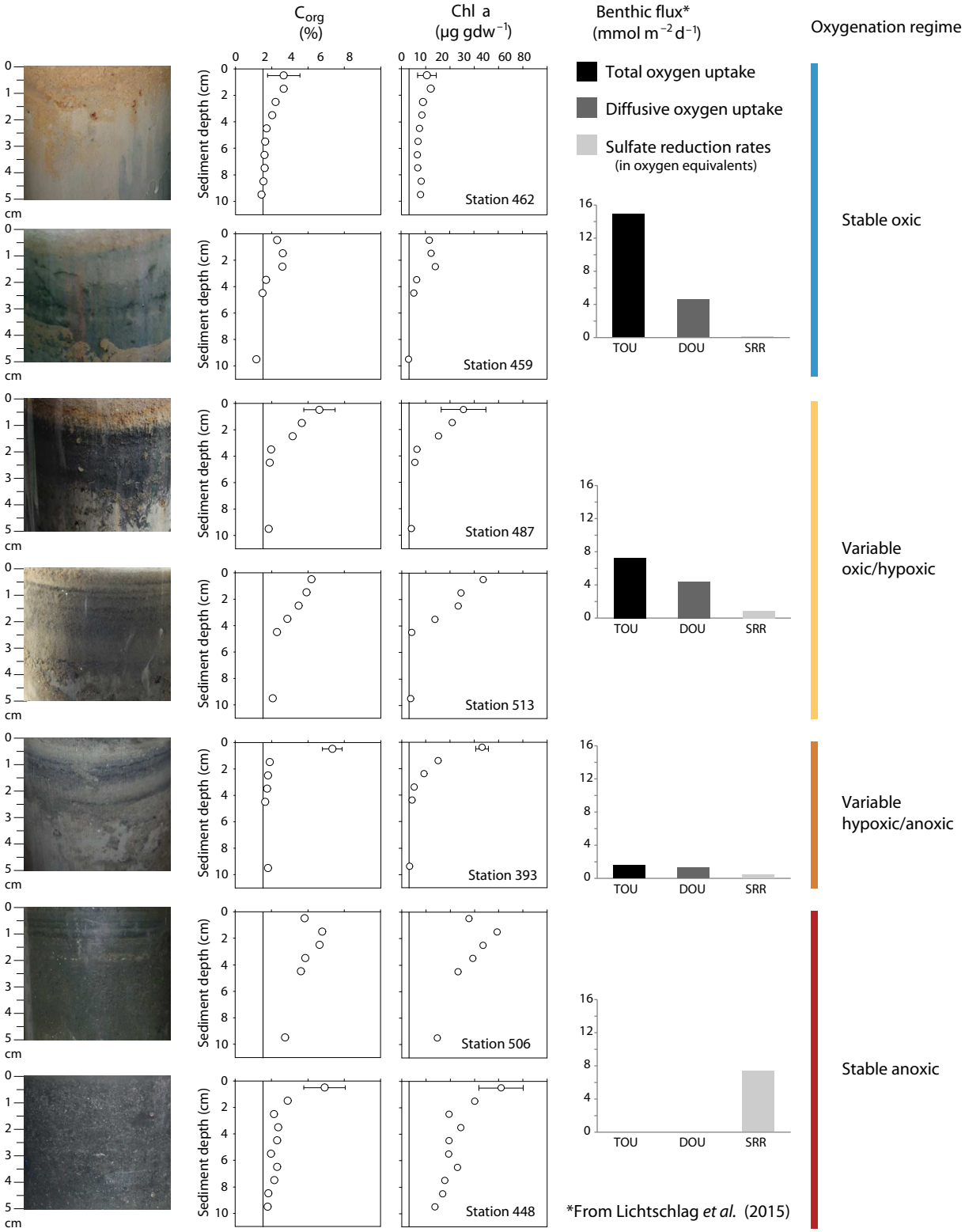

Fig. 2. Sediment organic matter content and benthic fluxes. Surface sediments sampled by coring and respective percentage of organic carbon and chlorophyll a (Chl a) concentration downcore (*y* axis is depth in cm; core pictures depict top 5 cm). The vertical line at ~1.6% C_{org} and ~3 µg gdw^{-1} Chl a depicts the lowest C_{org} and chlorophyll a contents in samples obtained, assumed to be the threshold for remineralization in the time frame of 40 years [based on ^{210}Pb; (*37*)]. Benthic fluxes (*37*), including sulfate reduction rates, are in oxygen equivalents (1:2 transformation). Color code depicts oxygenation regimes.

Table 1. Biogeochemistry of surface sediments (0 to 1 cm). Methane was around 1 to 2 nM, sulfate concentrations ranged between 13 and 17 μM, and molar organic carbon to nitrogen ratio was between 9.3 and 11.4 (mol/mol), without a specific trend (not shown). Values represent average and SD (n = 3) when available. In the case of acridine orange direct count (AODC), SD is based on counts of >100 squares on two replicate filters. Only oxic stations presented signs of bioturbation based on fauna abundances, shape of oxygen profiles, and microtopography [see Lichtschlag *et al.* (*37*) for details]. Range for faunal abundances is based on three to six replicate samples [integrated over the upper 5 cm; (*37*)]. C_{org}, organic carbon; C_{org}:N, molar C_{org}/N ratio; CPE, chloroplast pigment equivalents; THAA, surface and integrated concentrations over 0 to 5 cm in square brackets; DI, THAA-based degradation index; SRR, sulfate reduction rate; AODC, total cell counts based on AODC; < d.l., value below detection limit.

Station/ PANGAEA event label	Location (latitude/ longitude)	Water depth (m)	C_{org} (%)	Chlorophyll a (μg gdw^{-1})	CPE (μg gdw^{-1})	THAA (μmol gdw^{-1} [mmol m^{-2}])	DI	Fe^{2}+* (μM)	PO_4^{3}–* (μM)	Sulfide† (μM)	SRR* (nmol ml^{-1} day^{-1})	AODC (10^9 cells cm^{-3} sediment)	Macrofauna* (×10^3 individuals m^{-2})	Meiofauna* (×10^4 individuals m^{-2})
462 MSM15/ 1_462-1	44°49.45′N 33°9.26′E	105	2.6 ± 1.7	11 ± 4	19	16.0 ± 4.2 (754)	0.6 ± 0.1	84	3	< d.l.	<d.l.	2.5 ± 0.2	5–6.7	138–273.4
459 MSM15/ 1_459-1	44°40.48′N 33°5.53′E	120	2.9	12	37	15.7 (845)	1.3	—	—	—	—	—	50.8	199.5
487 MSM15/ 1_487-1	44°38.78′N 33°0.25′E	136	4.6 ± 0.9	26 ± 9	64 ± 19	23.5 ± 9.5 (796)	1.1 ± 0.3	21	5	< d.l.	14 ± 8	2.2 ± 0.0	26.3–51.4	172.2–226.3
513 MSM15/ 1_513-1	44°37.87′N 32°57.22′E	147	4.2	34	82	13.7 (730)	1.7	—	—	—	—	—	2.4	109.5
393 MSM15/ 1_393-1	44°37.08′N 32°53.48′E	164	5.3 ± 0.5	32 ± 2	86 ± 4	34.1 ± 11.7 (773)	1.3 ± 0.1	14	7	< d.l.	15 ± 10	1.9 ± 0.1	1.2	5.0
506 MSM15/ 1_506-1	44°36.38′N 32°52.72′E	171	3.8	29	66	23.4 (1396)	1.7	—	—	—	—	—	0	—
448 MSM15/ 1_448-1	44°35.84′N 32°49.03′E	207	4.9 ± 1.1	41 ± 9	94 ± 16	24.9 ± 3.4 (1289)	1.5 ± 0.5	< d.l.	3	92	83 ± 45	2.4 ± 0.4	0	0.13

*Data from Lichtschlag *et al.* (*37*). †Total sulfide concentration from upper 2 cm.

was ca. 10 μg gram dry weight (dw)$^{-1}$ at the oxic site but more than 40 μg gdw^{-1} at the anoxic site. When including detrital phaeopigments, a similar trend was observed ($F_{3,9}$ = 20.41, P < 0.001; Tukey post hoc test, P < 0.01), with the highest concentrations found under anoxic conditions (more than 90 μg gdw^{-1}). Chlorophyll a averaged 43 ± 7.2% of the sum of the pigments (chlorophyll a + phaeopigments), indicating the deposition of relatively fresh algal detritus at all sites. Chlorophyll a contents decreased with sediment depth, to a threshold of 3 μg gdw^{-1}, but remained fourfold higher in subsurface sediments of the hypoxic-anoxic sites ($F_{7,44}$ = 16.83, P < 0.001; Tukey post hoc test, P < 0.001; Fig. 2).

Other organic compounds and amino acid–based degradation index.

Total organic carbon (C_{org}) ranged between 2.6 and 5.3% dry weight in the top first centimeter, decreasing to ca. 1.6% with increasing sediment depth (Fig. 2). A further decrease was observed only in longer sediment cores, with a minimum in C_{org} content of 1.3% (fig. S2). Surface and downcore concentrations were substantially higher under hypoxic and anoxic conditions ($F_{7,60}$ = 24.12, P < 0.001; Tukey post hoc test, P < 0.01; Fig. 2, fig. S2, and Table 1), with a peak concentration at the chemocline (water depth of 150 m, 5% C_{org}). C_{org}:N ratio ranged from 9 to 11 in the different zones, with slightly lower values at the hypoxic stations. Total hydrolyzable amino acids (THAAs) were lower at the oxic station (Table 1 and fig. S3), and highest in variable hypoxic conditions with THAA of >30 μmol gdw^{-1} ($F_{3,11}$ = 3.72, P < 0.05; Tukey post hoc test, P < 0.05), whereas integrated values (0 to 5 cm) showed the highest concentrations under permanent anoxic conditions (Table 1 and fig. S4), suggesting further accumulation with time in the absence of oxygen.

The degradation index (DI) based on protein amino acids (*39*, *40*) averaged 1.2 ± 0.4 and ranged from 0.6 to 1.7, increasing along the transect from oxic to anoxic conditions (Table 1). The most degraded material (the lowest score) was found at the site exposed to highest oxygen availability, while the index of sites under anoxia indicated an accumulation of less degraded material ($F_{3,8}$ = 8.65, P < 0.005; Tukey post hoc test, P < 0.05). This trend was also observed downcore (fig. S3).

Dissolved organic matter.

Dissolved organic carbon and total dissolved nitrogen in pore water. The concentration and composition of pore-water dissolved organic carbon (DOC) are summarized in Table 2. Higher DOC concentrations were observed under oxic (387 μM) than in anoxic (275 μM) conditions, while total dissolved nitrogen (TDN) concentrations were greater in anoxic than in oxic conditions (81 and 58 μM, respectively). Accordingly, the DOC/TDN ratios of the dissolved organic matter (DOM) accumulating in pore water also differed, with ratios of 6.6 and 3.4 at the oxic and anoxic sites, respectively.

Table 2. DOM composition in pore waters as obtained from Fourier transform ion cyclotron resonance mass spectrometry analysis (pooled pore-water volume from 0 to 10 cm). Molecular weight for the molecules detected ranged from 406 to 461. Hydrogen and oxygen to carbon ratio (intensity weight average) ranged from 1.2 to 1.3 and 0.4 to 0.5, respectively. Almod, aromaticity index; DBE, double-bond equivalents; total CHO, CHON, and CHOP, percentage of formulae containing carbon, hydrogen, and phosphorus; total S-bearing compounds, percentage of formulae containing sulfur-bearing compounds.

	DOC (μM) and extraction efficiency (%)	TDN (μM) and extraction efficiency (%)	DOC/TDN molar ratio	Group of formulae	No. of formulae	$Almod_{wa}$	DBE_{wa}	Total CHO	Total CHON	Total CHOP	Total S-bearing compounds
Oxic	387 (51%)	58 (12%)	6.6	Exclusive oxic	678	0.2	8.8	33	45	28	17
Anoxic	275 (80%)	81 (10%)	3.4	Exclusive anoxic	626	0.3	9.3	14	27	12	57
				Common formulae	5287	0.2	7.4	37	39	1	22

DOM molecular characterization.

DOM in the pore water of the oxic and anoxic zones showed a high similarity in identified formulae (~89% shared), with ~11% of formulae unique to each condition. Nitrogen-containing compounds (CHON) represented 45% of exclusive formulae of the oxic site compared to 27% of the anoxic site (Table 2).

Under anoxic conditions, threefold more sulfur-bearing compounds (CHOS, CHONS, and CHOSP) were detected than in oxic conditions (57 and 19%, respectively), consistent with higher sulfurization ratios of organic matter, leading to the buildup of sulfurized DOM (fig. S5). Most sulfurized molecular formulae were unique for anoxic conditions (234 versus 69 formulae; fig. S5). Anoxic conditions showed a higher proportion of unsaturated molecular formulae (132 formulae) than sediments exposed to oxic bottom-water conditions (47 formulae), while molecular groups associated with fresh organic matter, such as unsaturated aliphatics, contributed 9 and 16 formulae, respectively. Only a minor contribution of sulfurized formulae associated with sugars was detected (<3 formulae).

Microbial community characterization

Cell abundance.

Cell abundance averaged $2.2 \pm 0.3 \times 10^9$ cells cm^{-3} sediment, without a clear trend related to bottom-water oxygen (Table 1). Subsurface sediments (2 to 4 cm) exposed to the most oxic bottom water conditions showed only negligibly higher cell abundance (3.5×10^9 cells cm^{-3}) than those in the most anoxic water conditions (3×10^9 cells cm^{-3}) (fig. S6). Below the top 5 cm, cell numbers decreased to less than half of those in the top sediments and then further decreased with increasing sediment depth but with minor differences across the sampling sites (fig. S6).

Bacterial community structure based on ARISA fingerprinting.

A total of 411 different operational taxonomic units (OTUs) were detected by automated ribosomal intergenic spacer analysis (ARISA) fingerprinting across all samples (sediment depth of 0 to 1 cm), with numbers ranging from 145 ± 9 to 187 ± 11 at each station along the transect (table S1). In the top seafloor layer exposed to different bottom-water oxygenation conditions, the number of distinct OTUs was significantly (17%) lower in permanent oxic sites than in sites with variable oxygenation regimes ($F_{3,80} = 6.21$, $P < 0.001$; Tukey post hoc test, $P < 0.01$; table S1). Overall, ca. 41 to 58% of OTUs detected were present at all sites. The permanently oxic zone (station 462) had no unique OTUs at all (table S1), but its bacterial community structure was still significantly different from that of communities at sites with variable and stable anoxic conditions [analysis of similarity (ANOSIM), Bonferroni-corrected, $P < 0.005$; table S1]. The nonmetric multidimensional scaling (NMDS) ordination plot (based on Bray-Curtis distance matrix of OTU relative abundances) indicated significant differences in bacterial community structure for all zones, with a grouping of stations according to their oxygenation regimes (ANOSIM, Bonferroni-corrected, $P < 0.005$; Fig. 3A).

Bacterial community structure based on 454 next-generation sequencing.

To explore the identity of the bacterial members of the benthic community, we carried out 454 next-generation sequencing (NGS) analysis of surface sediments from each oxygenation regime (stations 462, 487, 393, and 448; table S2), yielding a total of 35,783 sequence reads. These consisted of 4670 unique OTUs (97% clustering; hereafter referred to as $OTUs_{0.03}$), from which 50% were absolute singletons, that is, they consisted of only one sequence in the entire data set. These represented less than 6% of the total sequence reads and were not included in subsequent analyses. Across all sites, the percentage of shared OTUs was around 16 to 27%; accordingly, the estimate of dissimilarity (beta diversity; Bray-Curtis) was higher than that detected by ARISA because of the high proportion of rare taxa that ARISA does not detect. However, NGS analysis also indicated that the oxic microbial community was most different from the anoxic community, and the hypoxic-anoxic communities were more similar to each other and to the anoxic microbial community (table S2). Overall, the observed $OTUs_{0.03}$ number and estimated richness increased with decreasing concentration of oxygen in bottom waters (table S2). An increase in evenness (more even relative OTU abundance) was detected for permanent oxic and anoxic conditions (inverse Simpson index; $1/D$, 18 to 46), with an up to sixfold difference under variable hypoxic regimes. This trend was not limited to the oxic-anoxic gradient across the four zones, but was also seen the vertical profile with sediment depth in the oxic-hypoxic zones (table S2).

Two phyla, *Bacteroidetes* and *Proteobacteria*, clearly dominated the data set, and comprised ca. 43 and 27% of all reads, respectively. Among these, the most sequence-abundant OTUs belonged to *Deltaproteobacteria*, *Gammaproteobacteria*, and *Flavobacteriia* (Fig. 3B), which were, by far, the most abundant bacterial classes, representing ca. 60% of all sequences, with 40% occurring in all zones, similar to the pattern predicted by ARISA for abundant taxa. At the level of individual $OTU_{0.03}$, these groups shared <20% of all reads between the different oxygen regimes (table S3), suggesting niche differentiation along bottom-water oxygenation gradient.

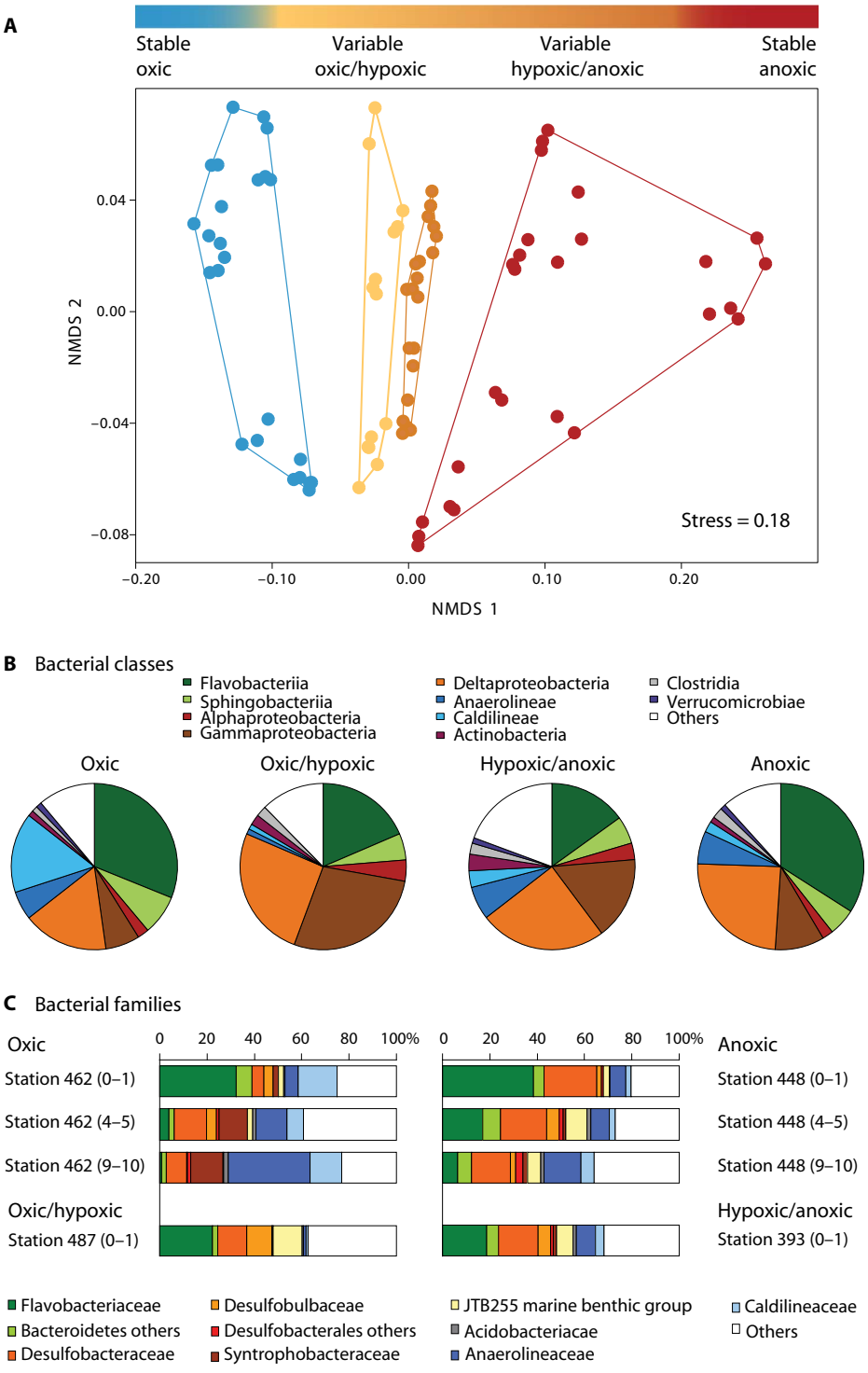

Fig. 3. Bacterial community structure in surface sediments. (**A**) NMDS ordination plot (Bray-Curtis distance matrix) of ARISA profiles for the sampling stations for surface sediments (0 to 1 cm below sea floor). Different colors represent different oxygenation regimes: blue, stable oxic; yellow, variable oxic-hypoxic; orange, variable anoxic-hypoxic; red, stable anoxic. Stress, 0.18. (**B**) Relative sequence abundance of bacterial classes across oxygenation regimes detected by 454 NGS. (**C**) Most abundant bacterial families in different sediment horizons [depth layer in parentheses (cm)]. Note that the term "oxic" refers to bottom-water oxygen concentration and not oxygen content in the sediments.

Caldilineae and *Anaerolineae* dominated the oxygenated zone, but their relative sequence abundance decreased with decreasing oxygen availability (Fig. 3, B and C). Also, the sequence abundances of bacterial taxa affiliated with *Flavobacteriia* decreased from >28% under stable oxic and anoxic conditions to <18% under variable oxygenation regimes. Approximately 15% of the $OTUs_{0.03}$ showed a linear increase (linear correlation coefficient $R > 0.8$) in relative sequence abundance with increasing anoxic conditions (table S4). For example, *Deltaproteobacteria* increased from 15% under permanent oxic conditions to 23 to 25% of all sequences at each site under variable to anoxic conditions. Notably, closely related OTUs were associated specifically with different oxygen concentrations (table S4): Some taxa reached the highest sequence abundances under variable hypoxic conditions, decreasing again toward stable oxic and anoxic conditions (Fig. 3B). These taxa included *Gammaproteobacteria*, whose relative abundances increased from <9% (in the case of permanent oxic and anoxic regimes) to 27% (under variable hypoxic conditions). The most abundant gammaproteobacterial family was affiliated with the JTB255 marine benthic group and followed the same trend. The 20 most sequence-abundant $OTUs_{0.03}$, representing more than ca. 30% of all reads, were dominated by *Lutimonas* (*Flavobacteriales*, 5.4%), unclassified *Syntrophobacteraceae* (2.8%), and *Desulfobulbus* (*Desulfobacterales*, 2.7%) (table S5), all of which showed a decrease in relative sequence abundance with increasing hypoxia.

Effect of hypoxia on different compartments of the ecosystem

Partial least squares path modeling (PLSPM) analysis was conducted to quantify direct versus indirect effects of oxygen availability (bottom-water oxygen concentration) on organic matter composition, remineralization, and diversity of metazoans and bacteria (Fig. 4). The final model of PLSPM analysis showed that bottom-water oxygen had a strong positive effect on bioturbation ($P < 0.001$), metazoan diversity ($P < 0.001$), faunal respiration ($P < 0.001$), and microbial aerobic respiration ($P < 0.001$) and a negative direct effect on organic matter accumulation (C_{org}, chlorophyll a, and THAA; marginally significant

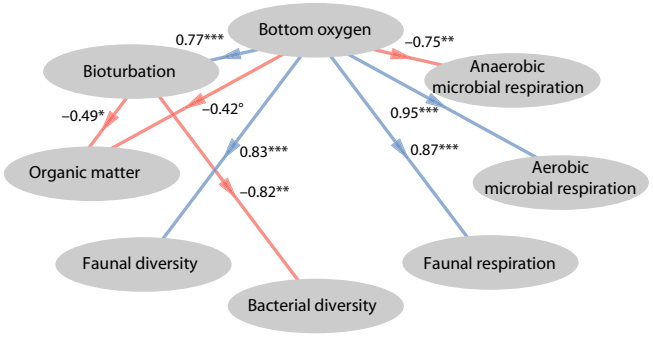

Fig. 4. Path diagram for the final model examining causal effects between bottom-water oxygen concentration (exogenous variable) and the endogenous variables: Organic matter (C_{org}, chlorophyll a, and THAA), bioturbation, macrofaunal and meiofaunal diversity (based on inverse Simpson index), faunal and microbial aerobic and anaerobic respiration [from Lichtschlag *et al*. (*37*)], and bacterial diversity (based on inverse Simpson index from ARISA). Arrows (paths) indicate negative (red) or positive (blue) effects of bottom-water oxygen concentration, respectively, and numbers associated with arrows represent path coefficients. The goodness-of-fit index of the model was 0.75. *P < 0.05; **P < 0.01; ***P < 0.001. °P = 0.08, marginally significant trend.

P = 0.08) and microbial anaerobic respiration (P < 0.01). Microbial diversity (based on inverse Simpson index) and organic matter accumulation were negatively affected by bioturbation (P < 0.01 and marginally significant P = 0.08, respectively). Bottom-water oxygen had no significant direct effect on microbial diversity (Fig. 4). Multivariate variation partitioning analysis showed that bottom-water oxygenation regime directly explained only 11% (P < 0.001) of community variation (top surface layer based on ARISA fingerprinting), consistent with the spread of ARISA OTUs, as assessed by correspondence analysis (fig. S7).

DISCUSSION

Bottom-water oxygen availability is one of the key factors governing the biogeochemistry and community composition of shelf and slope sediments (*10*). Previous studies have shown that with decreasing bottom-water oxygen concentrations, more organic matter can accumulate in marine sediments over a wide range of time scales (*11*, *41*). Even labile organic matter components can be preserved in anoxic sediments such as phytodetritus pigments, fatty acids (FAs), and amino acids (*9*, *10*). The underlying mechanisms and thresholds have remained controversial. Experimental studies often do not detect such effects (*15*), which could be due to their restricted duration or to artificial conditions such as dilution and mixing of sediments. In contrast, the interpretation of field data compilations is challenged by the lack of essential geochemical data to assess burial efficiency such as particle input, sediment accumulation rates, and oxygen exposure time. Here, we have sampled a persistent natural gradient in bottom-water oxygen concentrations within a transect of 40 km on the northwestern Crimean shelf break (Black Sea) and compared ecosystem-level functions across four zones: (i) permanent oxic, (ii) variable oxic-hypoxic, (iii) variable anoxic-hypoxic, and (iv) permanent anoxic, with sulfide in bottom waters.

Hypoxia and organic matter preservation

Surface sediment organic carbon and nitrogen content along the 40-km transect fell within the range described for surficial sediments of the Black Sea (*42*–*44*) and other hypoxic ecosystem at similar water depths and sedimentation rates [for example, depth of 140 m, Pakistan margin oxygen minimum zone; (*45*)]. THAA concentrations (Table 1) agreed with the range of data reported for surficial sediments of the Black Sea (*46*) and from the oxygen minimum zone of the Chilean upwelling coast (*47*) at similar water depths. Comparing surface sediments across the four zones of bottom-water oxygen availability, we observed an increasing preservation of organic matter with decreasing bottom-water oxygen concentration (Figs. 1 and 2 and Table 1), with a threshold already at the onset of hypoxia (bottom-water oxygen concentration of <63 μM O_2).

Our results indicate that even short-term hypoxic conditions, that is, exposure of seafloor sediments to a few days of hypoxic waters advected by internal waves can contribute to substantial carbon accumulation (Fig. 2 and Table 1). This was observed as an increase of total organic matter deposition by 50% over the same sediment depth interval, over a period of at least 40 years according to the burial rate (*37*). This pattern is consistent with the decline in rates of total oxygen uptake (diffusive and fauna-mediated oxygen uptake; Fig. 2), which decreased by the same magnitude (50%) toward hypoxic conditions, along with significant changes in the composition of megafauna and macrofauna. Bottom-water oxygen showed one of the strongest negative effects on both faunal diversity and respiration (Fig. 4 and table S6). The remineralization rate in oxygen equivalents, including reoxidation of, for example, sulfide, dropped fourfold between the variable oxic-hypoxic and hypoxic-anoxic zones (*37*). Our results confirm a tight coupling between oxygen availability, faunal activity, and organic matter remineralization (Fig. 4), showing that even short-term hypoxia causes substantial shifts in ecosystem function, leading to preservation of bulk organic matter. This is a relevant finding not only for the past history of anoxia in aquatic systems but also with regard to the future of seafloor ecosystems under oxygen stress, because physical transport of low-oxygen bottom waters by internal waves, eddies, and currents can substantially expand the area affected by hypoxia.

At the site with oxic bottom waters, minimum background C_{org} values of <1.6% were reached in the anoxic horizon at a sediment depth of 4 cm. Because of bioturbation at this site, this value represents a reccurring exposure to oxic-suboxic conditions over ca. 40 years according to the burial rates. In contrast, C_{org} concentrations were significantly higher in the hypoxic-anoxic zones (Fig. 2), which had much less fauna and lacked bioturbation (*37*). Organic carbon content remained at 1.9 to 2% (sediment depth of 2 to 4 cm) within 20 to 40 years, after which no further decline was observed, even down to a sediment depth of 70 cm (fig. S2), equivalent to a few hundred years. This confirms that a substantial fraction of organic matter escapes remineralization in the absence of bioturbation.

To further test the hypothesis of an influence of bottom-water oxygen availability on fauna and also on microbial community activity and structure and on the degradation rates and composition of organic matter, we assessed the accumulation of specific, presumably labile compounds, such as hydrolyzable amino acids, and phytodetrital chloroplastic pigments. Enhanced preservation of amino acids in sediments exposed to stable hypoxic conditions has previously been reported for the Pakistan margin oxygen minimum zone (*45*) and the Arabian Sea (*9*). Here, we could show that THAA accumulated already at the onset of hypoxia (<63 μM O_2) (Table 1) to concentrations above a threshold of 23 μmol gdw^{-1}. Integrated values over the depth layer of 0 to 5 cm suggest that a range of THAA can be preserved over hundreds of years under permanent anoxic conditions (Table 1).

Following the study of Dauwe *et al.* (*40*), we calculated the DI (THAA-based degradation index) based on the ratio of amino acids in sedimentary organic matter. As expected, DI values along the transect showed higher degradation (lowest score) at the site exposed to highest oxygen availability, while the index for sites under lower oxygenation regimes indicated that fresher material was buried (Table 1), in agreement with results from other marine environments subjected to permanent or seasonal hypoxia and anoxia (*9*, *45*). Our data fell in the range described for coastal sediments [(*40*) and references therein] and coastal areas exposed to seasonal oxygen minimum conditions at comparable depths (*47*). From the amino acid data set of Mopper *et al.* (*46*) for the Black Sea sediments exposed to permanent anoxic-sulfidic conditions, we also calculated positive DI scores of 1.2, in agreement with our results.

Similarly, more chloroplast pigments accumulated in the sediments with increasing hypoxia. We can exclude differential productivity regimes or export fluxes within the sampled transect as a cause for this pattern (fig. S1). Under oxic conditions, chlorophyll a pigments were already substantially degraded at the sediment surface (Fig. 2), confirming the relevance of faunal processing of sediments for the degradation of pigments and other organic compounds (*6*, *48*). Chlorophyll a preservation and total chloroplast pigments increased already at <63 and <100 μM O_2, respectively, in bottom waters. Chloroplast pigments increased by 200% under variable hypoxia and up to 300% under anoxia (Fig. 2 and Table 1). Overall, pigment concentrations were in the range of the oxygen minimum zone of the Chilean upwelling system (*49*) and the Pakistan margin (*50*), with a similar trend of lower concentrations accumulating in oxic waters compared to anoxic ones.

One hypothesis for the decrease of microbial remineralization efficiency under hypoxia and anoxia is the lack of particle grinding and mixing by benthic fauna [(*6*) and references therein)], which our model confirmed (Fig. 4). Furthermore, it has previously been suggested that sulfurization (also referred to as vulcanization) of lipids and carbohydrates through inorganic sulfur incorporation (*1*) could enhance carbon preservation in anoxic sediments. When oxygen is fully consumed, sulfate becomes the major electron acceptor in anoxic marine sediments, leading to the production of hydrogen sulfide. The relatively high sulfate reduction rates measured at the anoxic site and the amount of free hydrogen sulfide in pore waters of the subsurface layers (Table 1) suggest that sulfurization may have taken place in the absence of bioturbation. It was previously shown that, for anoxic Black Sea sediments, sulfurization of organic matter can occur during the very early stages of sedimentary diagenesis and even at the sediment-water interface (*51*). Our study assessed the sulfur signature of the DOM pool and found that anoxic conditions resulted in a threefold greater accumulation of sulfur-bearing compounds in the pore-water DOM pool (CHOS, CHONS, and CHOSP) than in sediments exposed to oxic bottom water (57 and 19%, respectively; Table 2). These results are consistent with previous findings on the sulfurization of sedimentary particulate and DOM under anoxia (*52*) that can be expressed by the sulfurization ratio, a proxy to assess the extent of sulfurization (fig. S5).

Effects on benthic bacterial communities under varying oxygen availability

A strong effect of oxygen on microbial community structure has recently been reported for pelagic ecosystems exposed to low oxygen concentration (*53*); changes in beta diversity were detected even at 50% oxygen undersaturation, at oxygen levels much higher than that defined as hypoxia. In contrast, the variation of oxygen in bottom waters showed a rather weak effect on the benthic bacterial diversity and community composition in the Baltic Sea sediments (*54*). In this first study of a persistent hypoxia gradient on microbial community composition in outer shelf sediments, we found a low direct effect of different bottom-water oxygen concentrations at the microbial diversity level, assessed as benthic bacterial sequence evenness (table S2) and composition (Fig. 3B), with two different fingerprinting methods targeting abundant types at low resolution (ARISA) or rare types at high resolution (454 NGS). Sequence diversity tended to increase with decreasing bottom-water oxygen and increasing sediment depth; this pattern could be explained by a greater number of unique, rare OTUs in anoxic sediments (tables S1 and S2). Nonetheless, we detected significant differences between the total community structure and individual groups of bacteria according to oxygen concentrations in the bottom water. Along the environmental gradient studied here, the most abundant classes overlapped among all sites, even at the $OTU_{0.03}$ level, up to 40% (table S3). However, for each OTU we could also identify different sequence-abundant ecotypes whose relative abundances were either positively or negatively associated with decreasing bottom-water oxygen concentration (table S5). This suggests that oxygen availability in bottom waters is a key factor in the selection and diversification of ecotypes of bacteria in suboxic to anoxic sediments, as studied here.

In the Black Sea sediments, more than 80% of the total sequences retrieved belonged to *Bacteroidetes* and *Proteobacteria* (41 and 42%, respectively), differing somewhat from the global composition of coastal sediments in the high fraction of *Bacteroidetes* (*55*). The most abundant bacterial groups at the class level were represented by *Deltaproteobacteria* and *Flavobacteriia*. These increased in sequence abundance toward anoxic conditions (Fig. 3, B and C), especially the group of sulfate-reducing bacteria affiliated with *Desulfobacteraceae* and *Desulfobulbaceae* (*Deltaproteobacteria*). Accordingly, sulfate reduction dominated organic matter remineralization with increasing hypoxia (Fig. 2 and Table 1), in agreement with previous investigations in the Black Sea (*33*, *43*, *56*) and in the upwelling ecosystem off central Chile (*57*) and with predicted changes in ecosystem function with hypoxia (*58*). Other abundant inhabitants of hypoxic conditions were affiliated with *Flavobacteriaceae* (*Flavobacteriia*) (Fig. 3, B and C), which comprised, by far, the most sequence-abundant bacterial family in this study, with ca. 15% of all NGS sequences. The high overlap of $OTU_{0.03}$ affiliated with *Flavobacteriia* between different oxygenation regimes suggests that this group, with its hydrolytic/fermentative capabilities, metabolic versatility, and copiotrophic characteristics (*59*–*61*), might be able to adapt well to varying oxygen conditions, supporting its dominance in organic-rich sediments exposed to variable oxygenation states (*62*, *63*). High relative abundances of *Flavobacteriaceae* were associated with the hypoxic zone, where labile organic matter accumulated in this study (Figs. 2 and 3C). Thus, *Flavobacteriaceae* present key community members under varying hypoxic conditions and could be referred to as part of a typical oxic-hypoxic microbiome, as it has been proposed for the planktonic relatives of this order, inhabiting pelagic oxygen minimum zones (*64*).

It had previously been suggested that the water column oxycline is biogeochemically similar to the sediment redox zone (*65*). However, other than the dominance of *Flavobacteriia*, we found few similarities between the most abundant taxa populating these two zones in the Black Sea. Published data show that dominant groups inhabiting the upper Black Sea hypoxic waters are affiliated with *Alphaproteobacteria* (mainly, SAR11), whereas *Gammaproteobacteria* (SUP05; *Methylococaceae*) and marine group A become more abundant toward anoxic conditions (*66*–*69*). Of these relevant groups in the pelagic chemocline, <0.1% were represented in the benthic hypoxic-anoxic zone. Rather, the microbial community of the

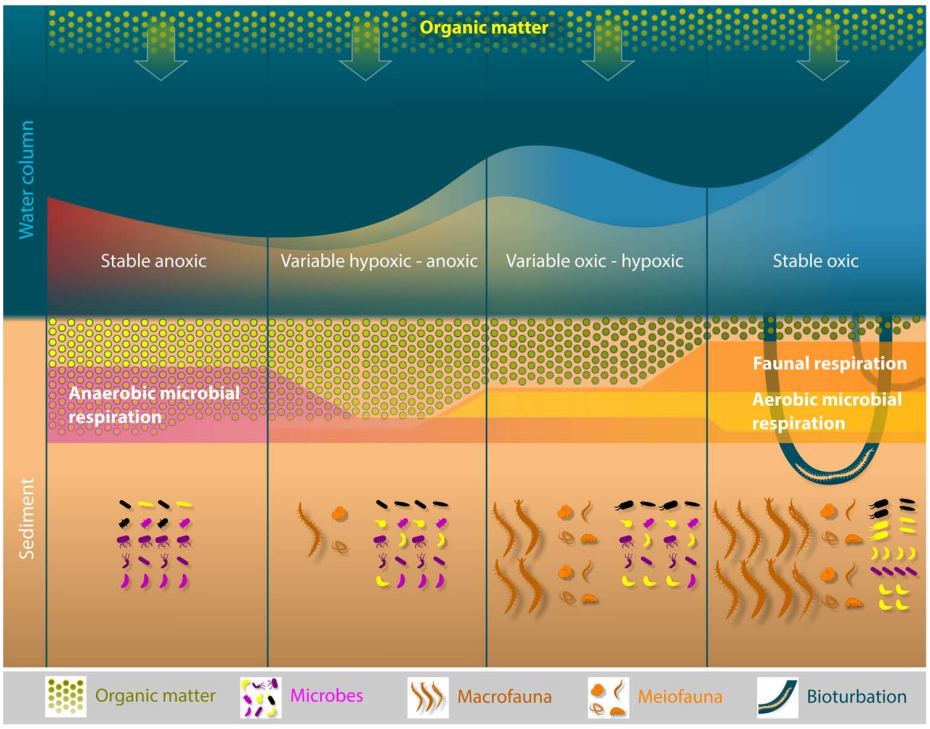

Fig. 5. Conceptual diagram of ecosystem processes changing with bottom-water oxygen on the northwestern Crimean shelf break (Black Sea). The filled areas (blue to red) show the minimum and maximum bottom-water oxygen or sulfide concentrations (see Fig. 1 for details) to which deposited organic matter (green circles) is exposed at the seafloor, leading to different remineralization rates. Diverse benthic communities inhabit the sediments, from fauna (macrofauna and meiofauna) to microbes, driving different functions in the ecosystem (see Fig. 4 for details on causal effects). Under stable oxic conditions, faunal abundance and bioturbation activity are high, leading to high aerobic respiration rates in all size classes (orange and yellow filled areas). At the onset of hypoxia, faunal respiration decreases and lack of bioturbation favors anaerobic microbial communities and processes such as sulfate reduction (purple filled area), increasing free hydrogen sulfide in pore waters of the subsurface layers and enhancing carbon preservation in anoxic sediments.

benthic chemocline was comprised of taxa affiliated with *Chloroflexi* (*Anaerolineae* and *Caldilineae*), candidate division JS1, and *Deltaproteobacteria* (*Desulfobacterales*), which dominate surface and subsurface sediments (*70*–*72*). Sulfide oxidizers were also found in some locations (*73*).

Factors influencing remineralization efficiencies: The role of oxygen in biogeochemical functioning of benthic communities

Our data support the hypothesis that a key factor in declining remineralization efficiencies with decreasing oxygen supply is the loss of faunal activity, such as feeding, bioturbation, and bioirrigation, by bottom-dwelling animals (*10*, *37*). Furthermore, we were able to quantify the substantial negative effect of short-term hypoxia on remineralization. In shelf areas and at the upper margin, the benthic fauna contribute a significant fraction of total remineralization rates (*74*), because of their specific abilities as multicellular organisms to efficiently feed on particles, move, collect, and redistribute food, and by their ability to transport oxygen into the sediments by bioturbation and bioirrigation. In hypoxic and anoxic zones of shelf seas, the diversity and biomass of benthic fauna decline because of oxygen limitation, as does their role in remineralization (*14*). Thus, as oxygen decreases, organic matter degradation increasingly depends on the activity of anaerobic microbes [for example, fermentation and sulfate reduction; (*10*, *75*)]. Previous investigations suggested that bacterial diversity and community composition can be affected by bioturbation (*76*, *77*). The bacterial community seems able to adapt rapidly to varying oxygen conditions but will respond to the decrease in fauna-mediated particle transport and milling with decreasing remineralization efficiencies. The reduction in organic matter and sediment mixing also explains the preservation even of labile organic matter fractions because microorganisms depend on diffusion in the absence of fauna.

Lichtschlag and colleagues (*37*) showed that both the abundance and richness of macrofauna and meiofauna decreased sharply along the transect from oxic to anoxic conditions. In contrast to faunal biodiversity, microbial diversity and evenness investigated in this study increased toward anoxic conditions (table S2), suggesting that these microbial variables cannot serve as indicators, to assess effects of hypoxia on the state of marine ecosystems. Our results support hypotheses based on patterns observed in pelagic and benthic ecosystems (*26*, *27*, *53*, *65*, *78*, *79*), which explain a higher microbial diversity in steep redox gradients and anoxic environments by the presence of a multitude of electron donor-acceptor couples, selecting for a variety of metabolic pathways and increasing the number of niches. The increase in microbial diversity with decreasing oxygen seen in this study (tables S1 and S2) may be linked to increasing anaerobic activity, including production and reoxidation of sulfide and ammonium and other products (table S4) (*37*). This is consistent with the hypothesis that under oxic conditions, many bacteria can fully mineralize the hydrolytic products to carbon dioxide, whereas in the absence of oxygen, organic matter breakdown is performed by diverse consortia of anaerobes (*4*, *80*, *81*), which have a lower energy yield and slower growth rates but very little grazing pressure in the absence of oxygen and could hence sustain a higher diversity.

CONCLUSIONS

A key question with relevance to past, present, and future states of coastal seas and the oceans concerns the effects of expanding hypoxia on marine ecosystem functioning. As summarized in Fig. 5, we have shown that variations in bottom-water oxygen supply, even when only leading to temporary hypoxia during a few days, can substantially enhance the preservation of organic matter for time scales of decades. This effect is best explained by the decrease in faunal abundance and activity at the onset of hypoxia, which leads to lower bioturbation rates and favors anaerobic microbial communities and processes such as fermentation and sulfate reduction. In the absence of particle mixing, even labile organic matter can accumulate for decades. Furthermore, variations in oxygen supply to the seafloor influenced the composition

of the bacterial community of surface sediments, with different selection pressures on closely related bacterial taxa.

MATERIALS AND METHODS

Sampling scheme

Seven stations were sampled across the northwestern Crimean shelf spanning a water depth of 105 to 207 m (Fig. 1). Sediments were collected by a video-guided multiple corer (TV-MUC; 96–mm–inner diameter core tubes) and a gravity corer (GC; 63–mm–inner diameter core tubes) during the MSM 15-1 expedition to the Black Sea (*RV Maria S. Merian*, Crimean Leg; 25 April 2010 to 7 May 2010; Table 1). Undisturbed sediment cores were sliced at intervals of 1 cm and processed for further analysis at in situ temperature of about 8°C. Sampling sites and their respective labels are summarized in Fig. 1 and Table 1 (http://dx.doi.org/10.1594/PANGAEA.855872).

Before each TV-MUC/GC deployment, a conductivity-temperature-depth (CTD) cast [SBE 911plus, with additional sensors for oxygen (SBE43) and fluorescence (ECO-AFL/FL; WET Labs)] was obtained to characterize the water column. Additional data of bottom-water oxygen and sulfide concentrations were obtained from Lichtschlag *et al.* (*37*), measured by oxygen sensors mounted to a benthic boundary layer profiler and the submarine JAGO or measured from Niskin bottles. Oxygen measurements from the CTD were calibrated by Winkler titration method (*82*). A detection limit of 2 µM was defined for water-column oxygen and sulfide concentrations, according to Lichtschlag *et al.* (*37*). Oxygen data are deposited at https://doi.pangaea.de/10.1594/PANGAEA.780438, https://doi.pangaea.de/10.1594/PANGAEA.780450, and http://dx.doi.org/10.1594/PANGAEA.740088.

Biogeochemical sediment analyses

Samples for organic carbon and nitrogen, pigments [chlorophyll a and its degradation products, in the sum chloroplast pigment equivalents (CPE)], and THAA were measured in triplicate for selected stations on freeze-dried and homogenized sediments retrieved from three different cores at stations 462, 487, 393, and 448 (Table 1) and from single cores at the remaining stations.

Sediment organic carbon and nitrogen were measured using a Fisons NA-1500 elemental analyzer. SDs were better than 0.2%. For organic carbon determination, samples were pretreated with 12.5% HCl to remove inorganic carbon. Chlorophyll a and CPE were measured spectrophotometrically according to Schubert *et al.* (*83*). THAAs were measured after Pantoja and Lee (*47*) from ca. 100 mg of sediment samples. Briefly, after hydrolysis (6 M HCl at 105°C for 21 hours under N_2 gas), the supernatant was removed and neutralized (6 M KOH). Amino acid identification and quantification were performed using high-performance liquid chromatography after precolumn derivatization with *o*-phthaldialdehyde and 2-mercaptoethanol according to previous studies (*84*, *85*). The DI of organic matter, depicting selective diagenetic alteration of sedimentary amino acids, was used as a proxy for the lability of sediment organic matter (*39*, *40*).

DOM analysis was performed on pore-water samples extracted with Rhizons (pore size of <0.2 µm; Rhizosphere Research Products) (*86*). Sediments under end-member conditions (oxic and anoxic) were assessed by extracting the section (0 to 10 cm) of the cores (using 108 and 77 ml of pore water for oxic and anoxic conditions, respectively). DOC and TDN concentrations were analyzed via catalytic oxidation at a high temperature on a TOC-VCPH Shimadzu instrument (*87*) on both the original pore-water samples and the solid phase–extracted samples. Solid phase–extracted DOC and TDN were determined on the methanol extracts after evaporation overnight and further dissolution in ultrapure water (pH 2) and used to calculate the extraction efficiency. The accuracy of the analysis was corroborated by analyzing deep seawater from the Consensus Reference Material Project (http://yyy.rsmas.miami.edu/groups/biogeochem/Table1.htm).

Pore-water samples were solid phase–extracted using 1 g of styrene divinyl benzene polymer column (Varian PPL) before mass spectrometric analysis, according to Dittmar *et al.* (*88*). Molecular analyses were performed at the Research Group for Marine Biogeochemistry (ICBM, Germany) by direct infusion into an ultrahigh-resolution 15-T Fourier transform ion cyclotron resonance mass spectrometer (Bruker solariX) equipped with an electrospray ionization (Apollo II Bruker Daltonik GmbH) source in a negative-ion mode. Formula assignments were accomplished for mass peaks with a signal-to-noise ratio of >4 and based on previously reported criteria (*89*). A molecular formula represents the chemical composition of a molecule based on the number of atoms of each element present ($C_cH_hN_nO_oS_s$) and is obtained on the basis of accurate mass determination but cannot be directly related to a chemical structure. Thus, molecular formulae were organized into different molecular groups, which have been recently shown to provide a good overview on the molecular composition of the samples (*90*, *91*). Molecular groups considered in DOM characterization were as follows: (i) formulae of unsaturated aliphatics ($1.5 < H/C < 2$, $O/C < 0.9$, and $N = 0$); (ii) peptide molecular formulae ($1.5 < H/C < 2$, $O/C < 0.9$, and $N > 0$); (iii) saturated FAs ($H/C > 2$ and $O/C < 0.9$), without (saturated FAs) or with heteroatoms (N, S, or P) (saturated FA-CHO_x); (iv) formulae of sugars ($O/C > 0.9$), without (sugars) and with heteroatoms (sugars-CHO_x); (v) highly unsaturated compounds (AImod < 0.5 and $H/C < 1.5$); (vi) polyphenols ($0.67 \geq$ AImod > 0.5); and (vii) condensed aromatics or dissolved black carbon (DBC; AImod ≥ 0.67), represented by three subgroups, with either <15 (DBC < 15C) or ≥15 (DBC ≥ 15C) C atoms both without and with heteroatoms (DBC-CHO_x). Molecular information of DOM was also evaluated on the basis of the contribution of CHO, CHON, CHOS, CHOP, and CHONS formulae in each sample and by the intensity weighted average (wa) of the elemental ratios H/C_{wa} and O/C_{wa}, as well as the double-bond equivalents (DBE_{wa}) and aromaticity index ($AImod_{wa}$) (*92*–*94*).

The sulfurization index was calculated after the study of Schmidt *et al.* (*52*) following Eq. 1

$$\frac{C_cH_{h+2}O_{0-1}\,S_1 + C_cH_{h+4}O_{0-2}S_2}{C_cH_hO_0} \quad (1)$$

where $C_cH_hO_0$ is the potential precursor of the sulfurization reaction, in which, for the incorporation of 1 S atom, 1 O atom is removed and 2 H atoms are added. A comprehensive characterization of pore-water geochemistry and sediment properties can be found at http://dx.doi.org/10.1594/PANGAEA.844879.

Benthic community characterization

Faunal community.

Abundance and composition of meiofauna and macrofauna were obtained from Lichtschlag *et al.* (*37*). Briefly, the upper 5 cm of each sediment core were sliced horizontally into 1-cm sections, washed through sieves of 1000- and 63-µm mesh sizes, and preserved in 75% alcohol. The animals retained in the size class of 1000 to 2000 µm were counted as macrofauna, while organisms retained in 63-µm mesh size were counted

as meiofauna. Animals were sorted and identified to higher taxa using a stereo microscope (×90 magnification) and a light microscope (up to ×1000 magnification).

Microbial community.

Cell counts. The number of cells in the sediments was determined at stations 462, 487, 393, and 448 by the AODC (Acridine Orange Direct Count) method. Subsampled 1 cm sediment sections were fixed in 2% formaldehyde-filtered artificial seawater, stored at 4°C, and treated according to previous studies (*95*, *96*). Total cell numbers were determined by randomly counting at least 30 grids per filter (for two replicate filters).

DNA extraction. Total community DNA was assessed from three different cores at each station. On board, sediment was subsampled and stored at −20°C for further analysis. Total DNA was extracted from ca. 1 g of wet sediment using UltraClean Soil DNA Isolation Kits (MO BIO Laboratories Inc.). Extracted DNA was quantified with a microplate spectrometer (Infinite 200 PRO NanoQuant; TECAN Ltd.), and its concentration was adjusted for each step of the subsequent molecular protocol.

Automated ribosomal intergenic spacer analysis. The bacterial community structure was determined by the ARISA fingerprinting method, according to Fisher and Triplett (*97*). Triplicate polymerase chain reactions from standardized amounts of DNA (10 ng) from each sample were amplified using the bacteria forward FAM-labeled ITSF and reverse ITSReub specific primers (*98*). All molecular protocols, including the binning into OTUs and data formatting, were carried out as described previously (*99*).

454 Next-generation sequencing. Extracted DNA was amplified and sequenced by the Research and Testing Laboratory (Lubbock, TX). The V4 to V6 regions of the 16*S* ribosomal RNA genes were amplified using the bacterial primers 530F and 1100R according to Klindworth *et al.* (*100*). Fragments were sequenced following the 454 pyrosequencing protocol (*101*) and Titanium reagent chemistry. The raw sequences and all the upstream workflow were conducted with mothur (v.1.29), following the standard operating procedure for chimera removing and clustering (*102*, *103*), including the implemented denoising algorithm. Sequence taxonomic assignments were carried out using the SILVA bacterial reference (*104*) downloaded from www.mothur.org (September 2013), and sequences were clustered at a 3% difference level into OTUs ($OTUs_{0.03}$). Sequence counts were standardized by the total amount of sequences per sample to get relative abundances, and singleton OTUs were removed. Sequences obtained in this study were deposited at the European Molecular Biology Laboratory under the project accession number PRJEB12983.

Statistical analysis. Data on respiration rates, bottom- and pore-water composition, and sulfate reduction rates that were included in the discussion and the statistical model of bottom-water oxygenation effects were previously published (*37*), and the respective data are available at doi:10.1594/PANGAEA.855872 and http://dx.doi.org/10.1594/PANGAEA.844879.

Statistical analysis was conducted following the study of Ramette (*105*) and using vegan and custom R scripts (*106*) performed in R (version 3.0.1; www.R-project.org). All diversity indexes for the 454 NGS data were obtained with mothur (v.1.29) (*102*). The associations between oxygen availability (bottom-water oxygen concentration), presence of bioturbation, metazoan diversity, organic matter, and faunal and microbial respiration with microbial community diversity were addressed using PLSPM (*107*) with the R package plspm, and only the final model is reported. Faunal and microbial respiration, together with abundance and composition of meiofauna and macrofauna, were obtained from Lichtschlag *et al.* (*37*). From the same data set, bioturbation was qualitatively deduced from a combination of fauna abundances, shape of oxygen profiles, and microtopography. For the path model, bottom-water oxygen was defined as an "exogenous" variable (that is, it is not expected to be affected by other variables in the model), whereas the rest were defined as "endogenous" variables (that is, their variances are partially explained by other variables in the model) (*107*).

SUPPLEMENTARY MATERIALS

Supplementary material for this article is available at http://advances.sciencemag.org/cgi/content/full/3/2/e1601897/DC1

table S1. Percentage of shared and total number of OTUs and ANOSIM based on Bray-Curtis distance matrix between oxygenation conditions (based on ARISA profiles, upper-left corner of the table).

table S2. Percentage of shared and total number of $OTU_{0.03}$ (based on 454 NGS, without singletons) between stations.

table S3. Pairwise comparisons based on OTU presence-absence (without singletons) between oxygenation regimes (at the $OTU_{0.03}$ level) for the three key bacterial groups: *Deltaproteobacteria* (up), *Gammaproteobacteria* (center), and *Flavobacteriia* (down).

table S4. Overview of 454 OTU sequences of relevant bacterial types responding to changes in bottom water oxygen concentration.

table S5. Ranking of most abundant bacterial OTUs (without singletons) in decreasing order of their relative sequence abundance (in %) across all samples.

table S6. Contribution (%) of each hypothesized relationship (path) to global explained variability [global R^2; see Tenenhaus *et al.* (*107*) for details].

table S7. Abundance of macrofauna and meiofauna taxa of the northwestern Crimean Shelf.

fig. S1. Ten years (5 May 2000 to 5 May 2010) of satellite-based surface chlorophyll a concentration.

fig. S2. Downcore organic carbon ($\%C_{org}$) in the upper 70 cm comparing permanent oxic (station 462, 105 m) and anoxic (station 448, 207 m) conditions on the Crimean shelf.

fig. S3. Downcore THAA concentrations (μmol gdw^{-1}) and DI comparing permanent oxic (station 462, 105 m) and anoxic (station 448, 207 m) conditions on the Crimean shelf.

fig. S4. THAA concentration integrated 0 to 5 cm (bars) and THAA surface concentrations (triangles).

fig. S5. Sulfurization ratio calculated for molecular formulae detected in pore waters extracted from oxic (A) and anoxic conditions (B).

fig. S6. Downcore cell abundances [single cells ($\times 10^9$) ml $sediment^{-1}$], in the upper 30 cm, comparing oxygen regimes on the Crimean shelf.

fig. S7. Ordination biplots generated by Correspondence Analysis (CA) of benthic communities retrieved on the Crimean shelf; (A) bacterial communities (based on ARISA fingerprinting), (B) meiofaunal and (C) macrofaunal abundances of each taxonomic group.

REFERENCES AND NOTES

1. D. J. Burdige, Preservation of organic matter in marine sediments: Controls, mechanisms, and an imbalance in sediment organic carbon budgets? *Chem. Rev.* **107**, 467–485 (2007).
2. S. Emerson, J. I. Hedges, Processes controlling the organic carbon content of open ocean sediments. *Paleoceanography* **3**, 621–634 (1988).
3. D. E. Canfield, Factors influencing organic carbon preservation in marine sediments. *Chem. Geol.* **114**, 315–329 (1994).
4. S. Arndt, B. B. Jørgensen, D. E. LaRowe, J. J. Middelburg, R. D. Pancost, P. Regnier, Quantifying the degradation of organic matter in marine sediments: A review and synthesis. *Earth-Sci. Rev.* **123**, 53–86 (2013).
5. M.-Y. Sun, R. C. Aller, C. Lee, S. G. Wakeham, Effects of oxygen and redox oscillation on degradation of cell-associated lipids in surficial marine sediments. *Geochim. Cosmochim. Acta* **66**, 2003–2012 (2002).
6. C. Lee, Controls on organic carbon preservation: The use of stratified water bodies to compare intrinsic rates of decomposition in oxic and anoxic systems. *Geochim. Cosmochim. Acta* **56**, 3323–3335 (1992).
7. R. C. Aller, Bioturbation and remineralization of sedimentary organic matter: Effects of redox oscillation. *Chem. Geol.* **114**, 331–345 (1994).
8. G. L. Cowie, S. Mowbray, M. Lewis, H. Matheson, R. McKenzie, Carbon and nitrogen elemental and stable isotopic compositions of surficial sediments from the Pakistan margin of the Arabian Sea. *Deep Sea Res. Part II* **56**, 271–282 (2009).
9. K. A. Koho, K. G. J. Nierop, L. Moodley, J. J. Middleburg, L. Pozzato, K. Soetaert, J. van der Plicht, G.-J. Reichart, Microbial bioavailability regulates organic matter preservation in marine sediments. *Biogeosciences* **10**, 1131–1141 (2013).

10. J. J. Middelburg, L. A. Levin, Coastal hypoxia and sediment biogeochemistry. *Biogeosciences* **6**, 1273–1293 (2009).
11. S. Katsev, S. A. Crowe, Organic carbon burial efficiencies in sediments: The power law of mineralization revisited. *Geology* **43**, 607–610 (2015).
12. N. N. Rabalais, W.-J. Cai, J. Carstensen, D. J. Conley, B. Fry, X. Hu, Eutrophication-driven deoxygenation in the coastal ocean. *Oceanography* **27**, 172–183 (2014).
13. F. J. R. Meysman, J. J. Middelburg, C. H. R. Heip, Bioturbation: A fresh look at Darwin's last idea. *Trends Ecol. Evol.* **21**, 688–695 (2006).
14. R. J. Diaz, R. Rosenberg, Spreading dead zones and consequences for marine ecosystems. *Science* **321**, 926–929 (2008).
15. L. Pozzato, D. van Oevelen, L. Moodley, K. Soetaert, J. J. Middelburg, Sink or link? The bacterial role in benthic carbon cycling in the Arabian Sea's oxygen minimum zone. *Biogeosciences* **10**, 6879–6891 (2013).
16. C. Van Colen, F. Rossi, F. Montserrat, M. G. I. Anderson, B. Gribsholt, P. M. J. Herman, S. Degraer, M. Vincx, T. Ysebaert, J. J. Middleburg, Organism-sediment interactions govern post-hypoxia recovery of ecosystem functioning. *PLOS ONE* **7**, e49795 (2012).
17. E. Kristensen, S. I. Ahmed, A. H. Devol, Aerobic and anaerobic decomposition of organic matter in marine sediment: Which is fastest? *Limnol. Oceanogr.* **40**, 1430–1437 (1995).
18. S. Okabe, P. H. Nielsen, W. L. Jones, W. G. Characklis, Sulfide product inhibition of *Desulfovibrio desulfuricans* in batch and continuous cultures. *Water Res.* **29**, 571–578 (1995).
19. B. E. van Dongen, S. Schouten, J. S. Sinninghe Damsté, Preservation of carbohydrates through sulfurization in a Jurassic euxinic shelf sea: Examination of the Blackstone Band TOC cycle in the Kimmeridge Clay Formation, UK. *Org. Geochem.* **37**, 1052–1073 (2006).
20. L. Moodley, J. J. Middelburg, H. T. S. Boschker, G. C. A. Duineveld, R. Pel, P. M. J. Herman, C. H. R. Heip, Bacteria and foraminifera: Key players in a short-term deep-sea benthic response to phytodetritus. *Mar. Ecol. Prog. Ser.* **236**, 23–29 (2002).
21. U. Witte, N. Aberle, M. Sand, F. Wenzhöfer, Rapid response of a deep-sea benthic community to POM enrichment: An in situ experimental study. *Mar. Ecol. Prog. Ser.* **251**, 27–36 (2003).
22. C. Bienhold, A. Boetius, A. Ramette, The energy-diversity relationship of complex bacterial communities in Arctic deep-sea sediments. *ISME J.* **6**, 724–732 (2012).
23. M. Jacob, T. Soltwedel, A. Boetius, A. Ramette, Biogeography of deep-sea benthic bacteria at regional scale (LTER HAUSGARTEN, Fram Strait, Arctic). *PLOS ONE* **8**, e72779 (2013).
24. D. E. Canfield, F. J. Stewart, B. Thamdrup, L. De Brabandere, T. Dalsgaard, E. F. Delong, N. P. Revsbech, O. Ulloa, A cryptic sulfur cycle in oxygen-minimum–zone waters off the Chilean coast. *Science* **330**, 1375–1378 (2010).
25. F. J. Stewart, O. Ulloa, E. F. DeLong, Microbial metatranscriptomics in a permanent marine oxygen minimum zone. *Environ. Microbiol.* **14**, 23–40 (2012).
26. O. Ulloa, D. E. Canfield, E. F. DeLong, R. M. Letelier, F. J. Stewart, Microbial oceanography of anoxic oxygen minimum zones. *Proc. Natl. Acad. Sci. U.S.A.* **109**, 15996–16003 (2012).
27. J. J. Wright, K. M. Konwar, S. J. Hallam, Microbial ecology of expanding oxygen minimum zones. *Nat. Rev. Microbiol.* **10**, 381–394 (2012).
28. E. Precht, M. Huettel, Rapid wave-driven advective pore water exchange in a permeable coastal sediment. *J. Sea Res.* **51**, 93–107 (2004).
29. B. Nikitine, The biological conditions of the Black Sea observed in 1923–25. *Nature* **116**, 863 (1925).
30. J. I. Sorokin, On the primary production and bacterial activities in the Black Sea. *J. Cons. Int. Explor. Mer.* **29**, 41–60 (1964).
31. D. A. Ross, E. T. Degens, J. MacIlvaine, Black Sea: Recent sedimentary history. *Science* **170**, 163–165 (1970).
32. D. M. Karl, Distribution, abundance, and metabolic states of microorganisms in the water column and sediments of the Black Sea. *Limnol. Oceanogr.* **23**, 936–949 (1978).
33. B. O. Thamdrup, R. A. Rosselló-Mora, R. Amann, Microbial manganese and sulfate reduction in Black Sea shelf sediments. *Appl. Environ. Microbiol.* **66**, 2888–2897 (2000).
34. J. W. Murray, K. Stewart, S. Kassakian, M. Krynytzky, D. DiJulio, in *The Black Sea Flood Question: Changes in Coastline, Climate, and Human Settlement*, V. Yanko-Hombach, A. S. Gilbert, N. Panin, P. M. Dolukhanov, Eds. (Springer, 2007), pp. 1–21.
35. E. V. Stanev, Y. He, J. Staneva, E. Yakushev, Mixing in the Black Sea detected from the temporal and spatial variability of oxygen and sulfide—Argo float observations and numerical modelling. *Biogeosciences* **11**, 5707–5732 (2014).
36. J. Friedrich, F. Janssen, D. Aleynik, H. W. Bange, N. Boltacheva, M. N. Çagatay, A. W. Dale, G. Etiope, Z. Erdem, M. Geraga, A. Gilli, M. T. Gomoiu, P. O. J. Hall, D. Hansson, Y. He, M. Holtappels, M. K. Kirf, M. Kononets, S. Konovalov, A. Lichtschlag, D. M. Livingstone, G. Marinaro, S. Mazlumyan, S. Naeher, R. P. North, G. Papatheodorou, O. Pfannkuche, R. Prien, G. Rehder, C. J. Schubert, T. Soltwedel, S. Sommer, H. Stahl, E. V. Stanev, A. Teaca, A. Tengberg, C. Waldmann, B. Wehrli, F. Wenzhöfer, Investigating hypoxia in aquatic environments: Diverse approaches to addressing a complex phenomenon. *Biogeosciences* **11**, 1215–1259 (2014).
37. A. Lichtschlag, D. Donis, F. Janssen, G. L. Jessen, M. Holtappels, F. Wenzhöfer, S. Mazlumyan, N. Sergeeva, C. Waldmann, A. Boetius, Effects of fluctuating hypoxia on benthic oxygen consumption in the Black Sea (Crimean shelf). *Biogeosciences* **12**, 5075–5092 (2015).
38. M. Grégoire, J. Friedrich, Nitrogen budget of the northwestern Black Sea shelf inferred from modeling studies and in situ benthic measurements. *Mar. Ecol. Prog. Ser.* **270**, 15–39 (2004).
39. B. Dauwe, J. J. Middelburg, Amino acids and hexosamines as indicators of organic matter degradation state in North Sea sediments. *Limnol. Oceanogr.* **43**, 782–798 (1998).
40. B. Dauwe, J. J. Middelburg, P. M. J. Herman, C. H. R. Heip, Linking diagenetic alteration of amino acids and bulk organic matter reactivity. *Limnol. Oceanogr.* **44**, 1809–1814 (1999).
41. J. I. Hedges, R. G. Keil, Sedimentary organic matter preservation: An assessment and speculative synthesis. *Mar. Chem.* **49**, 81–115 (1995).
42. S. E. Calvert, R. E. Karlin, L. J. Toolin, D. J. Donahue, J. R. Southon, J. S. Vogel, Low organic carbon accumulation rates in Black Sea sediments. *Nature* **350**, 692–695 (1991).
43. A. Weber, W. Riess, F. Wenzho, B. B. Jørgensen, Sulfate reduction in Black Sea sediments: In situ and laboratory radiotracer measurements from the shelf to 2000 m depth. *Deep Sea Res. Part I* **48**, 2073–2096 (2001).
44. G. L. Cowie, J. I. Hedges, in *Black Sea Oceanography*, E. İzdar, J. W. Murray, Eds. (Springer, 1991), pp. 343–359.
45. S. Vandewiele, G. Cowie, K. Soetaert, J. J. Middelburg, Amino acid biogeochemistry and organic matter degradation state across the Pakistan margin oxygen minimum zone. *Deep Sea Res. Part II* **56**, 376–392 (2009).
46. K. Mopper, W. Michaelis, C. Garrasi, E. T. Degens, in *Leg 42, Part 2, of the Cruises of the Drilling Vessel Glomar Challenger; Istanbul, Turkey, to Istanbul, Turkey, May-June 1975*, J. L. Usher, Ed. (Texas A&M University, Ocean Drilling Program, 1978), pp. 697–705.
47. S. Pantoja, C. Lee, Amino acid remineralization and organic matter lability in Chilean coastal sediments. *Org. Geochem.* **34**, 1047–1056 (2003).
48. C. Woulds, S. Bouillon, G. L. Cowie, E. Drake, J. J. Middelburg, U. Witte, Patterns of carbon processing at the seafloor: The role of faunal and microbial communities in moderating carbon flows. *Biogeosciences* **13**, 4343–4357 (2016).
49. D. Gutiérrez, V. A. Gallardo, S. Mayor, C. Neira, C. Vásquez, J. Sellanes, M. Rivas, A. Soto, F. Carrasco, M. Baltazar, Effects of dissolved oxygen and fresh organic matter on the bioturbation potential of macrofauna in sublittoral sediments off Central Chile during the 1997/1998 El Niño. *Mar. Ecol. Prog. Ser.* **202**, 81–99 (2000).
50. C. Woulds, G. L. Cowie, Sedimentary pigments on the Pakistan margin: Controlling factors and organic matter dynamics. *Deep Sea Res. Part II* **56**, 347–357 (2009).
51. S. G. Wakeham, J. S. Sinninghe Damsté, M. E. L. Kohnen, J. W. De Leeuw, Organic sulfur compounds formed during early diagenesis in Black Sea sediments. *Geochim. Cosmochim. Acta* **59**, 521–533 (1995).
52. F. Schmidt, B. P. Koch, M. Witt, K.-U. Hinrichs, Extending the analytical window for water-soluble organic matter in sediments by aqueous Soxhlet extraction. *Geochim. Cosmochim. Acta* **141**, 83–96 (2014).
53. R. L. Spietz, C. M. Williams, G. Rocap, M. C. Horner-Devine, A dissolved oxygen threshold for shifts in bacterial community structure in a seasonally hypoxic estuary. *PLOS ONE* **10**, e0135731 (2015).
54. A. K. Steenbergh, P. L. E. Bodelier, C. P. Slomp, H. J. Laanbroek, Effect of redox conditions on bacterial community structure in Baltic Sea sediments with contrasting phosphorus fluxes. *PLOS ONE* **9**, e92401 (2014).
55. L. Zinger, L. A. Amaral-Zettler, J. A. Fuhrman, M. Claire Horner-Devine, S. M. Huse, D. B. M. Welch, J. B. H. Martiny, M. Sogin, A. Boetius, A. Ramette, Global patterns of bacterial beta-diversity in seafloor and seawater ecosystems. *PLOS ONE* **6**, e24570 (2011).
56. B. B. Jørgensen, A. Weber, J. Zop, Sulfate reduction and anaerobic methane oxidation in Black Sea sediments. *Deep Sea Res. Part I* **48**, 2097–2120 (2001).
57. B. O. Thamdrup, D. E. Canfield, Pathways of carbon oxidation in continental margin sediments off central Chile. *Limnol. Oceanogr.* **41**, 1629–1650 (1996).
58. H. O. Pörtner, D. Karl, P. W. Boyd, W. Cheung, S. E. LluchCota, Y. Nojiri, D. Schmidt, P. Zavialov, Ocean systems, in *Climate Change 2014: Impacts, Adaptation, and Vulnerability. Part A: Global and Sectoral Aspects. Contribution of Working Group II to the Fifth Assessment Report of the Intergovernmental Panel of Climate Change*, C. B. Field, V. R. Barros, D. J. Dokken, K. J. Mach, M. D. Mastrandrea, T. E. Bilir, M. Chatterjee, K. L. Ebi, Y. O. Estrada, R. C. Genova, B. Girma, E. S. Kissel, A. N. Levy, S. Maccracken, P. R. Mastrandrea, L. L. White, Eds. (Cambridge Univ. Press, 2014).
59. J.-F. Bernardet, J. P. Bowman, The genus *Flavobacterium*, in *Volume 7: Proteobacteria: Delta, Epsilon Subclass*, M. Dworkin, S. Falkow, E. Rosenberg, K.-H. Schleifer, E. Stackebrandt, Eds. (Springer, 2006), pp. 481–531.
60. B. Köpke, R. Wilms, B. Engelen, H. Cypionka, H. Sass, Microbial diversity in coastal subsurface sediments: A cultivation approach using various electron acceptors and substrate gradients. *Appl. Environ. Microbiol.* **71**, 7819–7830 (2005).

61. B. A. McKew, A. J. Dumbrell, J. D. Taylor, T. J. McGenity, G. J. C. Underwood, Differences between aerobic and anaerobic degradation of microphytobenthic biofilm-derived organic matter within intertidal sediments. *FEMS Microbiol. Ecol.* **84**, 495–509 (2013).
62. E. M. Julies, V. Brüchert, B. M. Fuchs, M. Planck, M. Microbiology, Vertical shifts in the microbial community structure of organic-rich Namibian shelf sediments. *African J. Microbiol. Res.* **6**, 3887–3897 (2012).
63. H. Sinkko, K. Lukkari, L. M. Sihvonen, K. Sivonen, M. Leivuori, M. Rantanen, L. Paulin, C. Lyra, Bacteria contribute to sediment nutrient release and reflect progressed eutrophication-driven hypoxia in an organic-rich continental sea. *PLOS ONE* **8**, e67061 (2013).
64. O. Ulloa, J. J. Wright, L. Belmar, S. J. Hallam, in *The Prokaryotes—Prokaryotic Communities and Ecophysiology*, E. Rosenberg, E. F. DeLong, S. Lory, E. Stackebrandt, F. Thompson, Eds. (Springer Berlin Heidelberg, 2013), p. 528.
65. T. M. Fenchel, B. J. Finlay, Oxygen and the spatial structure of microbial communities. *Biol. Rev. Camb. Philos. Soc.* **83**, 553–569 (2008).
66. C. Vetriani, H. V. Tran, L. J. Kerkhof, Fingerprinting microbial assemblages from the oxic/anoxic chemocline of the Black Sea. *Appl. Environ. Microbiol.* **69**, 6481–6488 (2003).
67. C. J. Schubert, M. J. L. Coolen, L. N. Neretin, A. Schippers, B. Abbas, E. Durisch-Kaiser, B. Wehrli, E. C. Hopmans, J. S. S. Damsté, S. Wakeham, M. M. M. Kuypers, Aerobic and anaerobic methanotrophs in the Black Sea water column. *Environ. Microbiol.* **8**, 1844–1856 (2006).
68. P. Lam, M. M. Jensen, G. Lavik, D. F. McGinnis, B. Müller, C. J. Schubert, R. Amann, B. Thamdrup, M. M. Kuypers, Linking crenarchaeal and bacterial nitrification to anammox in the Black Sea. *Proc. Natl. Acad. Sci. U.S.A.* **104**, 7104–7109 (2007).
69. C. A. Fuchsman, J. B. Kirkpatrick, W. J. Brazelton, J. W. Murray, J. T. Staley, Metabolic strategies of free-living and aggregate-associated bacterial communities inferred from biologic and chemical profiles in the Black Sea suboxic zone. *FEMS Microbiol. Ecol.* **78**, 586–603 (2011).
70. J. Leloup, A. Loy, N. J. Knab, C. Borowski, M. Wagner, B. B. Jørgensen, Diversity and abundance of sulfate-reducing microorganisms in the sulfate and methane zones of a marine sediment, Black Sea. *Environ. Microbiol.* **9**, 131–142 (2007).
71. A.-M. Tanase, T. Vassu, C. Trasca, In situ visualization of natural microbial communities in Black Sea coastal shelf sediments. *Rom. Biotech. Lett.* **14**, 4187–4193 (2009).
72. A. Schippers, D. Kock, C. Höft, G. Köweker, M. Siegert, Quantification of microbial communities in subsurface marine sediments of the Black Sea and off Namibia. *Front. Microbiol.* **3**, 16 (2012).
73. G. L. Jessen, A. Lichtschlag, U. Struck, A. Boetius, Distribution and composition of thiotrophic mats in the hypoxic zone of the Black Sea (150-170m water depth, Crimea margin). *Front. Microbiol.* **7**, 1011 (2016).
74. R. N. Glud, Oxygen dynamics of marine sediments. *Mar. Biol. Res.* **4**, 243–289 (2008).
75. M. W. Bowles, J. M. Mogollón, S. Kasten, M. Zabel, K.-U. Hinrichs, Global rates of marine sulfate reduction and implications for sub–sea-floor metabolic activities. *Science* **344**, 889–891 (2014).
76. J. D. Taylor, M. Cunliffe, Polychaete burrows harbour distinct microbial communities in oil-contaminated coastal sediments. *Environ. Microbiol. Rep.* **7**, 606–613 (2015).
77. M. Yazdani Foshtomi, U. Braeckman, S. Derycke, M. Sapp, D. Van Gansbeke, K. Sabbe, A. Willems, M. Vincx, J. Vanaverbeke, The link between microbial diversity and nitrogen cycling in marine sediments is modulated by macrofaunal bioturbation. *PLOS ONE* **10**, e0130116 (2015).
78. C. Lasher, G. Dyszynski, K. Everett, J. Edmonds, W. Ye, W. Sheldon, S. Wang, S. B. Joye, M. Ann Moran, W. B. Whitman, The diverse bacterial community in intertidal, anaerobic sediments at Sapelo Island, Georgia. *Microb. Ecol.* **58**, 244–261 (2009).
79. V. M. Madrid, G. T. Taylor, M. I. Scranton, A. Y. Chistoserdov, Phylogenetic diversity of bacterial and archaeal communities in the anoxic zone of the Cariaco Basin. *Appl. Environ. Microbiol.* **67**, 1663–1674 (2001).
80. D. E. Canfield, E. Kristensen, B. O. Thamdrup, Aquatic geomicrobiology. *Adv. Mar. Biol.* **48**, 1–599 (2005).
81. C. Arnosti, C. Bell, D. L. Moorhead, R. L. Sinsabaugh, A. D. Steen, M. Stromberger, M. Wallenstein, M. N. Weintraub, Extracellular enzymes in terrestrial, freshwater, and marine environments: Perspectives on system variability and common research needs. *Biogeochemistry* **117**, 5–21 (2014).
82. L. W. Winkler, Die Bestimmung des im Wasser gelösten Sauerstoffes. *Ber. Dtsch. Chem. Ges.* **21**, 2843–2854 (1888).
83. C. J. Schubert, J. Niggemann, G. Klockgether, T. G. Ferdelman, Chlorin Index: A new parameter for organic matter freshness in sediments. *Geochem. Geophys. Geosyst.* **6**, Q03005 (2005).
84. P. Lindroth, K. Mopper, High performance liquid chromatographic determination of subpicomole amounts of amino acids by precolumn fluorescence derivatization with o-phthaldialdehyde. *Anal. Chem.* **51**, 1667–1674 (1979).
85. S. Pantoja, C. Lee, Peptide decomposition by extracellular hydrolysis in coastal seawater and salt marsh sediment. *Mar. Chem.* **63**, 273–291 (1999).
86. J. Seeberg-Elverfeldt, M. Schlüter, T. Feseker, M. Kölling, Rhizon sampling of porewaters near the sediment-water interface of aquatic systems. *Limnol. Oceanogr. Methods* **3**, 361–371 (2005).
87. A. Stubbins, T. Dittmar, Low volume quantification of dissolved organic carbon and dissolved nitrogen. *Limnol. Oceanogr. Methods* **10**, 347–352 (2012).
88. T. Dittmar, B. Koch, N. Hertkorn, G. Kattner, A simple and efficient method for the solid-phase extraction of dissolved organic matter (SPE-DOM) from seawater. *Limnol. Oceanogr. Methods* **6**, 230–235 (2008).
89. P. E. Rossel, A. V. Vähätalo, M. Witt, T. Dittmar, Molecular composition of dissolved organic matter from a wetland plant (*Juncus effusus*) after photochemical and microbial decomposition (1.25 yr): Common features with deep sea dissolved organic matter. *Org. Geochem.* **60**, 62–71 (2013).
90. M. Seidel, M. Beck, T. Riedel, H. Waska, I. G. N. A. Suryaputra, B. Schnetger, J. Niggemann, M. Simon, T. Dittmar, Biogeochemistry of dissolved organic matter in an anoxic intertidal creek bank. *Geochim. Cosmochim. Acta* **140**, 418–434 (2014).
91. P. E. Rossel, C. Bienhold, A. Boetius, T. Dittmar, Dissolved organic matter in pore water of Arctic Ocean sediments: Environmental influence on molecular composition. *Org. Geochem.* **97**, 41–52 (2016).
92. F. W. McLafferty, F. Turecek, *Interpretation of Mass Spectra* (University Science Books, ed. 4, 1993).
93. B. P. Koch, T. Dittmar, From mass to structure: An aromaticity index for high-resolution mass data of natural organic matter. *Rapid Commun. Mass Spectrom.* **20**, 926–932 (2006).
94. B. P. Koch, T. Dittmar, From mass to structure: An aromaticity index for high-resolution mass data of natural organic matter. *Rapid Commun. Mass Spectrom.* **30**, 250 (2016).
95. M. I. Velji, L. J. Albright, Microscopic enumeration of attached marine bacteria of seawater, marine sediment, fecal matter, and kelp blade samples following pyrophosphate and ultrasound treatments. *Can. J. Microbiol.* **32**, 121–126 (1986).
96. A. Boetius, K. Lochte, Effect of organic enrichments on hydrolytic potentials and growth of bacteria in deep-sea sediments. *Mar. Ecol. Prog. Ser.* **140**, 239–250 (1996).
97. M. M. Fisher, E. W. Triplett, Automated approach for ribosomal intergenic spacer analysis of microbial diversity and its application to freshwater bacterial communities. *Appl. Environ. Microbiol.* **65**, 4630–4636 (1999).
98. M. Cardinale, L. Brusetti, P. Quatrini, S. Borin, A. M. Puglia, A. Rizzi, E. Zanardini, C. Sorlini, C. Corselli, D. Daffonchio, Comparison of different primer sets for use in automated ribosomal intergenic spacer analysis of complex bacterial communities. *Appl. Environ. Microbiol.* **70**, 6147–6156 (2004).
99. A. Ramette, Quantitative community fingerprinting methods for estimating the abundance of operational taxonomic units in natural microbial communities. *Appl. Environ. Microbiol.* **75**, 2495–2505 (2009).
100. A. Klindworth, E. Pruesse, T. Schweer, J. Peplies, C. Quast, M. Horn, F. O. Glöckner, Evaluation of general 16S ribosomal RNA gene PCR primers for classical and next-generation sequencing-based diversity studies. *Nucleic Acids Res.* **41**, e1 (2012).
101. M. Margulies, M. Egholm, W. E. Altman, S. Attiya, J. S. Bader, L. A. Bemben, J. Berka, M. S. Braverman, Y.-J. Chen, Z. Chen, S. B. Dewell, L. Du, J. M. Fierro, X. V. Gomes, B. C. Godwin, W. He, S. Helgesen, C. H. Ho, G. P. Irzyk, S. C. Jando, M. L. I. Alenquer, T. P. Jarvie, K. B. Jirage, J.-B. Kim, J. R. Knight, J. R. Lanza, J. H. Leamon, S. M. Lefkowitz, M. Lei, J. Li, K. L. Lohman, H. Lu, V. B. Makhijani, K. E. McDade, M. P. McKenna, E. W. Myers, E. Nickerson, J. R. Nobile, R. Plant, B. P. Puc, M. T. Ronan, G. T. Roth, G. J. Sarkis, J. F. Simons, J. W. Simpson, M. Srinivasan, K. R. Tartaro, A. Tomasz, K. A. Vogt, G. A. Volkmer, S. H. Wang, Y. Wang, M. P. Weiner, P. Yu, R. F. Begley, J. M. Rothberg, Genome sequencing in microfabricated high-density picolitre reactors. *Nature* **437**, 376–380 (2005).
102. P. D. Schloss, S. L. Westcott, T. Ryabin, J. R. Hall, M. Hartmann, E. B. Hollister, R. A. Lesniewski, B. B. Oakley, D. H. Parks, C. J. Robinson, J. W. Sahl, B. Stres, G. G. Thallinger, D. J. Van Horn, C. F. Weber, Introducing mothur: Open-source, platform-independent, community-supported software for describing and comparing microbial communities. *Appl. Environ. Microbiol.* **75**, 7537–7541 (2009).
103. P. D. Schloss, D. Gevers, S. L. Westcott, Reducing the effects of PCR amplification and sequencing artifacts on 16S rRNA-based studies. *PLOS ONE* **6**, e27310 (2011).
104. E. Pruesse, C. Quast, K. Knittel, B. M. Fuchs, W. Ludwig, J. Peplies, F. O. Glöckner, SILVA: A comprehensive online resource for quality checked and aligned ribosomal RNA sequence data compatible with ARB. *Nucleic Acids Res.* **35**, 7188–7196 (2007).
105. A. Ramette, Multivariate analyses in microbial ecology. *FEMS Microbiol. Ecol.* **62**, 142–160 (2007).
106. J. Oksanen, G. Blanchet, R. Kindt, P. Legendre, B. O'Hara, G. L. Simpson, P. Solymos, H. H. Stevens, H. Wagner, vegan: Community Ecology Package (2010).

Science Advances

AAAS

advances.sciencemag.org/cgi/content/full/3/2/e1601897/DC1

Supplementary Materials for

Hypoxia causes preservation of labile organic matter and changes seafloor microbial community composition (Black Sea)

Gerdhard L. Jessen, Anna Lichtschlag, Alban Ramette, Silvio Pantoja, Pamela E. Rossel, Carsten J. Schubert, Ulrich Struck, Antje Boetius

Published 10 February 2017, *Sci. Adv.* **3**, e1601897 (2017)
DOI: 10.1126/sciadv.1601897

This PDF file includes:

- table S1. Percentage of shared and total number of OTUs and ANOSIM based on Bray-Curtis distance matrix between oxygenation conditions (based on ARISA profiles, upper-left corner of the table).
- table S2. Percentage of shared and total number of $OTU_{0.03}$ (based on 454 NGS, without singletons) between stations.
- table S3. Pairwise comparisons based on OTU presence-absence (without singletons) between oxygenation regimes (at the $OTU_{0.03}$ level) for the three key bacterial groups: *Deltaproteobacteria* (up), *Gammaproteobacteria* (center), and *Flavobacteriia* (down).
- table S4. Overview of 454 OTU sequences of relevant bacterial types responding to changes in bottom water oxygen concentration.
- table S5. Ranking of most abundant bacterial OTUs (without singletons) in decreasing order of their relative sequence abundance (in %) across all samples.
- table S6. Contribution (%) of each hypothesized relationship (path) to global explained variability [global R^2; see Tenenhaus *et al*. (*107*) for details].
- table S7. Abundance of macrofauna and meiofauna taxa of the northwestern Crimean Shelf.
- fig. S1. Ten years (5 May 2000 to 5 May 2010) of satellite-based surface chlorophyll a concentration.
- fig. S2. Downcore organic carbon ($\%C_{org}$) in the upper 70 cm comparing permanent oxic (station 462, 105 m) and anoxic (station 448, 207 m) conditions on the Crimean shelf.

- fig. S3. Downcore THAA concentrations (μmol gdw^{-1}) and DI comparing permanent oxic (station 462, 105 m) and anoxic (station 448, 207 m) conditions on the Crimean shelf.
- fig. S4. THAA concentration integrated 0 to 5 cm (bars) and THAA surface concentrations (triangles).
- fig. S5. Sulfurization ratio calculated for molecular formulae detected in pore waters extracted from oxic (A) and anoxic conditions (B).
- fig. S6. Downcore cell abundances [single cells ($\times 10^9$) ml $sediment^{-1}$], in the upper 30 cm, comparing oxygen regimes on the Crimean shelf.
- fig. S7. Ordination biplots generated by Correspondence Analysis (CA) of benthic communities retrieved on the Crimean shelf; (A) bacterial communities (based on ARISA fingerprinting), (B) meiofaunal and (C) macrofaunal abundances of each taxonomic group.

table S1. Percentage of shared and total number of OTUs and ANOISM based on Bray-Curtis distance matrix between oxygenation conditions (based on ARISA profiles, upper-left corner of the table). Data for the different oxygenation regimes, and 3 sediment horizons for each station. The lower triangle is the percentage of shared OTUs. The upper triangle is β-diversity (calculated as Bray-Curtis dissimilarity. Values represent average and standard deviation (±; n= 3 - 11) when available. Reciprocal of Simpson index (1/D). Values in parenthesis denotes *R* values, ** *P*<0.05, *** P<0.001 (after Bonferroni correction)

	Stable oxic	Oxic/hypoxic	Anoxic/hypoxic	Stable anoxic	462 (0-1)	462 (4-5)	462 (9-10)	459 (0-1)	459 (4-5)	459 (9-10)	487 (0-1)	487 (4-5)	487 (9-10)	513 (0-1)	513 (4-5)	513 (9-10)	393 (0-1)	393 (4-5)	393 (9-10)	506 (0-1)	506 (4-5)	448 (0-1)	448 (4-5)	448 (9-10)	No. of OTU	Unique OTU	1/D
Stable oxic		0.44±0.06	0.46±0.04	0.53±0.05																					**176±15**	**1**	**64±10**
Oxic/hypoxic	47±11(0.6***)		0.34±0.07	0.47±0.07																					**195±10**	**4**	**77±8**
Anoxic/hypoxic	48±7(0.8***)	58±8(0.4*)		0.46±0.05																					**194±9**	**3**	**80±8**
Stable anoxic	41±6 (0.8***)	48±8(0.6***)	49±9(0.6***)																						**183±23**	**7**	**60±21**
Stable oxic (462; 0-1 cm)						0.4±0.04	0.5±0.02	0.4±0.04	0.4±0.01	0.5±0.04	0.4±0.05	0.5±0.01	0.6±0.01	0.4±0.02	0.5±0.01	0.7±0.02	0.5±0.17	0.6±0.12	0.7±0.03	0.4±0.01	0.5±±0.02	0.5±0.03	0.5±0.03	0.5±0.01	**145±9**	**0**	**63±11**
Stable oxic (462; 4-5 cm)					54±4		0.4±0.07	0.4±0.03	0.3±0.08	0.4±0.06	0.5±0.07	0.4±0.02	0.6±0.03	0.5±0.02	0.5±0.03	0.6±0.04	0.5±0.11	0.5±0.13	0.7±0.04	0.5±0.02	0.4±0.02	0.6±0.04	0.5±0.03	0.5±0.02	**140±22**	**5**	**55±13**
Stable oxic (462; 9-10 cm)					44±1	48±6		0.5±0.03	0.4±0.04	0.3±0.1	0.5±0.06	0.3±0.06	0.5±0.05	0.5±0.02	0.5±0.05	0.6±0.03	0.6±0.08	0.5±0.1	0.7±0.02	0.5±0.02	0.4±0.02	0.6±0.03	0.6±0.03	0.5±0.02	**133±4**	**1**	**48±6**
Stable oxic (459; 0-1 cm)					55±4	48±2	41±1		0.4±0.05	0.5±0.03	0.4±0.04	0.5±0.03	0.6±0.01	0.3±0.03	0.5±0.03	0.6±0.01	0.5±0.16	0.6±0.1	0.7±0.02	0.4±0.04	0.4±0.02	0.5±0.04	0.5±0.04	0.5±0.01	**178±8**	**7**	**66±3**
Stable oxic (459; 4-5 cm)					52±3	59±8	50±4	49±5		0.4±0.07	0.5±0.09	0.3±0.03	0.6±0.02	0.5±0.03	0.5±0.04	0.6±0.03	0.5±0.1	0.5±0.16	0.7±0.02	0.5±0.03	0.4±0.02	0.6±0.04	0.5±0.03	0.5±0.01	**134±17**	**1**	**51±9**
Stable oxic (459; 9-10 cm)					43±4	50±5	58±8	41±2	53±6		0.5±0.06	0.3±0.06	0.5±0.01	0.5±0.02	0.5±0.03	0.6±0.01	0.5±0.06	0.6±0.09	0.6±0.03	0.6±0.02	0.4±0.02	0.6±0.03	0.6±0.03	0.5±0.04	**144±21**	**4**	**51±6**
Oxic/hypoxic (487; 0-1 cm)					49±5	43±7	40±5	55±4	44±10	40±5		0.5±0.07	0.6±0.04	0.3±0.05	0.6±0.05	0.7±0.04	0.5±0.18	0.6±0.1	0.7±0.03	0.3±0.05	0.4±0.1	0.4±0.05	0.4±0.06	0.4±0.07	**168±16**	**1**	**77±9**
Oxic/hypoxic (487; 4-5 cm)					44±2	51±3	53±6	42±3	54±4	57±6	42±6		0.4±0.02	0.5±0.02	0.4±0.05	0.5±0.01	0.5±0.07	0.5±0.12	0.6±0.03	0.5±0.01	0.4±0.04	0.6±0.03	0.5±0.04	0.4±0.03	**145±6**	**2**	**52±2**
Oxic/hypoxic (487; 9-10 cm)					27±1	34±2	40±3	27±2	33±2	41±1	28±4	45±3		0.6±0.01	0.5±0.01	0.5±0.04	0.6±0.05	0.5±0.02	0.6±0.02	0.7±0.01	0.5±0.02	0.7±0.02	0.7±0.02	0.5±0.02	**125±7**	**8**	**45±5**
Oxic/hypoxic (513; 0-1 cm)					53±5	45±3	42±2	60±4	47±6	40±2	60±6	45±4	29±1		0.5±0.04	0.7±0.02	0.4±0.23	0.6±0.11	0.7±0.01	0.3±0.01	0.4±±0.02	0.4±0.04	0.4±0.06	0.4±0.03	**176±21**	**0**	**77±7**
Oxic/hypoxic (513; 4-5 cm)					44±2	41±3	43±3	39±5	41±3	43±3	37±5	51±4	41±2	39±5		0.5±0.01	0.5±0.03	0.5±0.06	0.6±0.05	0.6±0.02	0.5±0.02	0.6±0.05	0.6±0.04	0.5±0.01	**167±54**	**11**	**57±25**
Oxic/hypoxic (513; 9-10 cm)					27±1	33±3	35±2	30±1	33±3	36±3	30±5	40±2	45±5	31±4	42±3		0.5±0.23	0.4±0.17	0.4±0.03	0.7±0.03	0.6±0.02	0.7±0.03	0.6±0.02	0.6±0.02	**146**	**3**	**46**
Anoxic/hypoxic (393; 0-1 cm)					41±8	39±8	39±7	42±6	40±8	40±5	44±8	42±7	36±5	49±4	41±4	46±16		0.5±0.16	0.5±0.18	0.5±0.28	0.5±0.17	0.5±0.17	0.5±0.2	0.5±0.17	**151±25**	**2**	**80±8**
Anoxic/hypoxic (393; 4-5 cm)					36±9	41±10	38±6	37±8	42±12	38±5	36±8	44±10	38±4	38±10	43±4	50±14	45±12		0.5±0.14	0.6±0.1	0.5±0.14	0.6±0.07	0.6±0.08	0.5±0.07	**147±11**	**12**	**48±6**
Anoxic/hypoxic (393; 9-10 cm)					26±3	29±5	29±3	28±2	31±2	31±3	29±4	35±3	35±1	27±2	36±6	48±3	39±14	44±11		0.7±0.02	0.6±0.02	0.7±0.03	0.7±0.04	0.6±0.03	**136±29**	**8**	**26±10**
Stable anoxic (506; 0-1 cm)					53±2	43±0	41±1	57±6	42±6	38±3	63±8	41±2	27±1	66±1	37±3	29±3	46±8	35±7	27±2		0.4±0.02	0.3±0.05	0.4±0.07	0.4±0.02	**182**	**2**	**64±0**
Stable anoxic (506; 4-5 cm)					49±1	49±1	44±2	49±1	52±4	47±1	50±10	51±4	36±3	52±1	42±4	37±3	47±17	40±11	31±4	49		0.5±0.03	0.4±0.02	0.3±±0.02	**166**	**3**	**56**
Stable anoxic (448; 0-1 cm)					46±3	41±3	39±2	51±4	42±5	39±3	55±5	42±3	29±2	54±5	39±4	33±3	45±6	36±5	28±3	63±7	47±2		0.4±0.05	0.5±0.04	**187±11**	**5**	**60±23**
Stable anoxic (448; 4-5 cm)					46±2	42±3	39±4	48±5	43±3	38±3	51±7	42±5	28±3	55±7	39±4	32±1	47±19	36±7	27±4	57±8	52±4	57±6		0.4±0.03	**170±22**	**2**	**64±18**
Stable anoxic (448; 9-10 cm)					47±0	46±2	43±3	50±3	48±2	46±2	52±7	53±3	34±3	53±4	46±0	40±3	50±19	41±5	32±4	53±3	62±3	53±4	60±4		**178±5**	**1**	**65±26**

table S2. Percentage of shared and total number of $OTU_{0.03}$ (based on 454 NGS, without singletons) between stations. Data for the different oxygenation regimes, and 3 sediment horizons for end member conditions oxic and anoxic. The lower part of the matrix represents percentage of shared OTUs. Upper the matrix diagonal depicts β-diversity (Bray-Curtis dissimilarity). Inverse Simpson index (1/D). The raw data (including singletons) for surface sediments comprised 35783 reads and 4670 $OTU_{0.03}$.

	462 (0-1)	**487 (0-1)**	**393 (0-1)**	**448 (0-1)**	462 (4-5)	462 (9-10)	448 (4-5)	448 (9-10)	**No. of OTU**	**No. of sequences**	**unique OTU**	**1/D**
Stable oxic (462; 0-1 cm)		0.68	0.66	0.69	0.65	0.75	0.71	0.72	523	5541	68	18
Oxic/hypoxic (487; 0-1 cm)	18		0.61	0.58	0.79	0.89	0.62	0.78	1258	9177	336	98
Anoxic/hypoxic (393; 0-1 cm)	17	27		0.64	0.64	0.75	0.51	0.58	1532	12483	328	114
Stable anoxic (448; 0-1 cm)	16	27	22		0.8	0.87	0.6	0.74	877	6505	140	38
Stable oxic (462; 4-5 cm)	20	12	20	12		0.57	0.71	0.63	773	5585	191	51
Stable oxic (462; 9-10 cm)	15	7	14	8	26		0.8	0.66	548	7082	132	46
Stable anoxic (448; 4-5 cm)	15	24	33	27	17	11		0.62	1198	6805	196	140
Stable anoxic (448; 9-10 cm)	18	13	26	18	21	22	24		808	3802	130	158

table S3. Pairwise comparisons based on OTU presence-absence (without singletons) between oxygenation regimes (at the $OTU_{0.03}$ level) for the three key bacterial groups: *Deltaproteobacteria* (up), *Gammaproteobacteria* (center), and *Flavobacteriia* (down). Upper triangle denotes β −diversity (calculated as Bray-Curtis dissimilarity) and the lower triangle the percentage of shared $OTU_{0.03}$.

Deltaproteobacteria	Stable oxic	Oxic/hypoxic	Anoxic/hypoxic	Stable anoxic
Stable oxic		0.6	0.6	0.8
Oxic/hypoxic	20		0.6	0.6
Anoxic/hypoxic	20	30		0.8
Stable anoxic	17	32	25	

Gammaproteobacteria	Stable oxic	Oxic/hypoxic	Anoxic/hypoxic	Stable anoxic
Stable oxic		0.8	0.7	0.4
Oxic/hypoxic	17		0.5	0.7
Anoxic/hypoxic	16	26		0.7
Stable anoxic	21	26	23	

Flavobacteriia	Stable oxic	Oxic/hypoxic	Anoxic/hypoxic	Stable anoxic
Stable oxic		0.6	0.7	0.4
Oxic/hypoxic	35		0.3	0.4
Anoxic/hypoxic	28	31		0.4
Stable anoxic	30	53	28	

table S4. Overview of 454 OTU sequences of relevant bacterial types responding to changes in bottom water oxygen concentration. Bacterial OTU (>0.1% of total sequence abundance) that showed a (A) linear increase or (B) decrease in relative sequence abundance with decreasing bottom water oxygen concentration across all stations (R >0.8).

(A) proportion of sequences increasing with decreasing bottom water oxygen

OTU ID	Phylum	Class	Order	Family	Genus
Otu00052	Actinobacteria	Actinobacteria	Actinobacteridae	Actinomycetales	Frankineae
Otu00009	Bacteroidetes	Flavobacteriia	Flavobacteriales	Flavobacteriaceae	Lutibacter
Otu00094	Bacteroidetes	Flavobacteriia	Flavobacteriales	Flavobacteriaceae	Sediminibacter
Otu00361	Bacteroidetes	Flavobacteriia	Flavobacteriales	Flavobacteriaceae	Flavobacterium
Otu00538	Bacteroidetes	Flavobacteriia	Flavobacteriales	Flavobacteriaceae	Polaribacter
Otu00559	Bacteroidetes	Sphingobacteriia	Sphingobacteriales	BD2-2	unclassified
Otu00662	Bacteroidetes	Sphingobacteriia	Sphingobacteriales	BD2-2	unclassified
Otu00668	Bacteroidetes	Sphingobacteriia	Sphingobacteriales	BD2-2	unclassified
Otu00685	Bacteroidetes	Flavobacteriia	Flavobacteriales	Flavobacteriaceae	Tenacibaculum
Otu00739	Bacteroidetes	Flavobacteriia	Flavobacteriales	Flavobacteriaceae	Lutibacter
Otu00800	Bacteroidetes	Sphingobacteriia	Sphingobacteriales	BD2-2	unclassified
Otu00841	Bacteroidetes	Flavobacteriia	Flavobacteriales	Flavobacteriaceae	NS5
Otu00969	Bacteroidetes	Sphingobacteriia	Sphingobacteriales	Rhodothermaceae	Rhodothermus
Otu01596	Bacteroidetes	Flavobacteriia	Flavobacteriales	Flavobacteriaceae	Muricauda
Otu01600	Bacteroidetes	Sphingobacteriia	Sphingobacteriales	WCHB1-69	unclassified
Otu01911	Bacteroidetes	Flavobacteriia	Flavobacteriales	Flavobacteriaceae	Ulvibacter
Otu02014	Bacteroidetes	Flavobacteriia	Flavobacteriales	Flavobacteriaceae	NS5
Otu03059	Bacteroidetes	Sphingobacteriia	Sphingobacteriales	Flammeovirgaceae	Flexithrix
Otu04821	Bacteroidetes	Sphingobacteriia	Sphingobacteriales	PHOS-HE51	unclassified
Otu00124	Bacteroidetes	Flavobacteriia	Flavobacteriales	Flavobacteriaceae	Actibacter
Otu00183	Bacteroidetes	Flavobacteriia	Flavobacteriales	Flavobacteriaceae	Lutibacter
Otu00329	Bacteroidetes	VC2.1	unclassified	unclassified	unclassified
Otu01382	Candidate_division_OD1	unclassified	unclassified	unclassified	unclassified
Otu00390	Candidate_division_OD1	unclassified	unclassified	unclassified	unclassified
Otu00586	Candidate_division_OD1	unclassified	unclassified	unclassified	unclassified
Otu03723	Candidate_division_OP3	unclassified	unclassified	unclassified	unclassified
Otu00875	Candidate_division_OP8	unclassified	unclassified	unclassified	unclassified
Otu00101	Candidate_division_TM6	unclassified	unclassified	unclassified	unclassified
Otu01498	Candidate_division_TM6	unclassified	unclassified	unclassified	unclassified
Otu04692	Candidate_division_TM6	unclassified	unclassified	unclassified	unclassified
Otu01182	Candidate_division_TM7	unclassified	unclassified	unclassified	unclassified
Otu02202	Candidate_division_WS1	unclassified	unclassified	unclassified	unclassified
Otu00799	Chloroflexi	Anaerolineae	Anaerolineales	Anaerolineaceae	uncultured_Anaerolineaceae
Otu01713	Chloroflexi	Caldilineae	Caldilineales	Caldilineaceae	uncultured_Caldilineaceae
Otu02236	Chloroflexi	Anaerolineae	Anaerolineales	Anaerolineaceae	uncultured_Anaerolineaceae
Otu04169	Chloroflexi	Anaerolineae	Anaerolineales	Anaerolineaceae	uncultured_Anaerolineaceae
Otu00102	Chloroflexi	Anaerolineae	Anaerolineales	Anaerolineaceae	unclassified
Otu00195	Chloroflexi	Anaerolineae	Anaerolineales	Anaerolineaceae	unclassified

Otu00071	Cyanobacteria	unclassified	unclassified	unclassified	unclassified
Otu00133	Cyanobacteria	unclassified	unclassified	unclassified	unclassified
Otu00488	Cyanobacteria	SubsectionIII	Halomicronema	unclassified	unclassified
Otu01693	Cyanobacteria	unclassified	unclassified	unclassified	unclassified
Otu02719	Cyanobacteria	unclassified	unclassified	unclassified	unclassified
Otu00095	Cyanobacteria	SHA-109	unclassified	unclassified	unclassified
Otu00760	Deferribacteres	Unclassified_Deferribacterales	LCP-89	unclassified	unclassified
Otu01505	Firmicutes	Clostridia	Clostridiales	Family_XVII_Incertae_Sedis	unclassified
Otu00327	Firmicutes	Clostridia	Clostridiales	Lachnospiraceae	Parasporobacterium-Sporobacterium
Otu00426	Firmicutes	Clostridia	Clostridiales	Clostridiaceae	Geosporobacter
Otu01452	Firmicutes	unclassified	Unclassified	unclassified	unclassified
Otu01785	Firmicutes	Bacilli	Lactobacillales	Aerococcaceae	Dolosicoccus
Otu01935	Firmicutes	Clostridia	Clostridiales	Veillonellaceae	Anaerospora
Otu00191	Hyd24-12	unclassified	unclassified	unclassified	unclassified
Otu02220	Hyd24-12	unclassified	unclassified	unclassified	unclassified
Otu01433	Nitrospirae	Nitrospira	Nitrospirales	0319-6A21	unclassified
Otu04063	NPL-UPA2	unclassified	unclassified	unclassified	unclassified
Otu00708	Planctomycetes	Phycisphaerae	Phycisphaerales	Phycisphaeraceae	CL500-3
Otu02645	Planctomycetes	Phycisphaerae	Phycisphaerales	Phycisphaeraceae	CL500-3
Otu01752	Planctomycetes	Phycisphaerae	SHA-43	unclassified	unclassified
Otu00370	Planctomycetes	MBMPE71	unclassified	unclassified	unclassified
Otu00012	Proteobacteria	Deltaproteobacteria	Desulfobacterales	Desulfobacteraceae	Desulfobacula
Otu00055	Proteobacteria	Deltaproteobacteria	Desulfobacterales	Desulfobacteraceae	Desulfobacula
Otu00099	Proteobacteria	Deltaproteobacteria	Desulfobacterales	Desulfobacteraceae	Desulfobacula
Otu00100	Proteobacteria	Deltaproteobacteria	Desulfobacterales	Desulfobacteraceae	Desulfobacterium
Otu00300	Proteobacteria	Deltaproteobacteria	Desulfobacterales	Desulfobacteraceae	Desulfobacterium
Otu00445	Proteobacteria	Deltaproteobacteria	Desulfobacterales	Desulfobacteraceae	Desulfobacterium
Otu00491	Proteobacteria	Deltaproteobacteria	Desulfobacterales	Desulfobacteraceae	Desulfobacula
Otu00511	Proteobacteria	Deltaproteobacteria	Desulfarculales	Desulfarculaceae	uncultured_Desulfarculaceae
Otu00588	Proteobacteria	Betaproteobacteria	TRA3-20	unclassified	unclassified
Otu00610	Proteobacteria	Gammaproteobacteria	unclassified	unclassified	unclassified
Otu00612	Proteobacteria	Deltaproteobacteria	Desulfarculales	Desulfarculaceae	uncultured_Desulfarculaceae
Otu01030	Proteobacteria	Betaproteobacteria	Methylophilales	Methylophilaceae	OM43
Otu01257	Proteobacteria	Gammaproteobacteria	JTB148	unclassified	unclassified
Otu01356	Proteobacteria	Deltaproteobacteria	Desulfobacterales	Desulfobacteraceae	unclassified
Otu01865	Proteobacteria	Gammaproteobacteria	JTB148	unclassified	unclassified
Otu02028	Proteobacteria	Deltaproteobacteria	Desulfobacterales	Desulfobacteraceae	Desulfococcus
Otu00132	Proteobacteria	Gammaproteobacteria	Legionellales	Legionellaceae	uncultured_Legionellaceae
Otu00291	Proteobacteria	Deltaproteobacteria	Desulfobacterales	Desulfobacteraceae	Desulfobacterium
Otu00337	Proteobacteria	Gammaproteobacteria	Alteromonadales	Pseudoalteromonadaceae	Algicola
Otu00484	Proteobacteria	Deltaproteobacteria	Desulfobacterales	Desulfobacteraceae	unclassified
Otu00601	Proteobacteria	Alphaproteobacteria	Caulobacterales	Hyphomonadaceae	Robiginitomaculum
Otu00649	Proteobacteria	Deltaproteobacteria	Desulfobacterales	Desulfobacteraceae	Desulfobacterium
Otu00657	Proteobacteria	Gammaproteobacteria	Thiotrichales	Piscirickettsiaceae	endosymbionts
Otu00719	Proteobacteria	Deltaproteobacteria	Sh765B-TzT-29	unclassified	unclassified
Otu00723	Proteobacteria	Gammaproteobacteria	Oceanospirillales	OM182	unclassified
Otu00733	Proteobacteria	Deltaproteobacteria	Sh765B-TzT-29	unclassified	unclassified
Otu00754	Proteobacteria	Alphaproteobacteria	Rhodobacterales	Rhodobacteraceae	uncultured_Rhodobacteraceae
Otu00810	Proteobacteria	Deltaproteobacteria	Desulfobacterales	Desulfobulbaceae	Desulfocapsa

Otu00843	Proteobacteria	Deltaproteobacteria	Desulfobacterales	Desulfobacteraceae	Desulfobacterium
Otu00870	Proteobacteria	Deltaproteobacteria	Sh765B-TzT-29	unclassified	unclassified
Otu01137	Proteobacteria	Gammaproteobacteria	Oceanospirillales	OM182	unclassified
Otu01256	Proteobacteria	Deltaproteobacteria	Desulfobacterales	Desulfobacteraceae	unclassified
Otu01392	Proteobacteria	Deltaproteobacteria	Desulfobacterales	Desulfobulbaceae	Desulfobacterium
Otu01464	Proteobacteria	Alphaproteobacteria	Rhodospirillales	Rhodospirillaceae	uncultured_Rhodospirillaceae
Otu01474	Proteobacteria	Deltaproteobacteria	Bdellovibrionales	Bdellovibrionaceae	OM27
Otu01689	Proteobacteria	Alphaproteobacteria	Rickettsiales	Anaplasmataceae	unclassified
Otu01778	Proteobacteria	Gammaproteobacteria	KI89A_clade	unclassified	unclassified
Otu01811	Proteobacteria	Alphaproteobacteria	Rhodobacterales	Rhodobacteraceae	Maritimibacter
Otu01815	Proteobacteria	Deltaproteobacteria	Sh765B-TzT-29	unclassified	unclassified
Otu02001	Proteobacteria	Gammaproteobacteria	Methylococcales	Methylococcaceae	Methylococcus
Otu02178	Proteobacteria	Gammaproteobacteria	Alteromonadales	Alteromonadaceae	OM60_NOR5_clade
Otu02404	Proteobacteria	Deltaproteobacteria	Desulfovibrionales	Desulfovibrionaceae	Desulfovibrio
Otu02419	Proteobacteria	Gammaproteobacteria	Thiohalophilus	unclassified	unclassified
Otu02424	Proteobacteria	Gammaproteobacteria	Legionellales	Coxiellaceae	Coxiella
Otu02500	Proteobacteria	Deltaproteobacteria	Desulfobacterales	Desulfobulbaceae	Desulfocapsa
Otu02633	Proteobacteria	Betaproteobacteria	Burkholderiales	Comamonadaceae	Caldimonas
Otu02887	Proteobacteria	Deltaproteobacteria	Desulfobacterales	Desulfobacteraceae	Desulfobacula
Otu02900	Proteobacteria	Gammaproteobacteria	Oceanospirillales	Oceanospirillaceae	Marinobacterium
Otu03125	Proteobacteria	unclassified	unclassified	unclassified	unclassified
Otu03268	Proteobacteria	Deltaproteobacteria	Myxococcales	Nannocystineae	Haliangiaceae
Otu04725	Proteobacteria	Deltaproteobacteria	Sh765B-TzT-29	unclassified	unclassified
Otu05020	Proteobacteria	Gammaproteobacteria	Thiotrichales	Piscirickettsiaceae	endosymbionts
Otu05103	Proteobacteria	Deltaproteobacteria	Desulfobacterales	Desulfobacteraceae	Desulfococcus
Otu05363	Proteobacteria	Gammaproteobacteria	Thiohalophilus	unclassified	unclassified
Otu05387	Proteobacteria	Gammaproteobacteria	Xanthomonadales	JTB255_marine_benthic_group	unclassified
Otu00176	Proteobacteria	Deltaproteobacteria	Desulfarculales	Desulfarculaceae	uncultured_Desulfarculaceae
Otu00206	Proteobacteria	Deltaproteobacteria	Desulfarculales	Desulfarculaceae	uncultured_Desulfarculaceae
Otu00258	Proteobacteria	Deltaproteobacteria	Desulfarculales	Desulfarculaceae	uncultured_Desulfarculaceae
Otu00566	Proteobacteria	Deltaproteobacteria	Desulfobacterales	Desulfobacteraceae	unclassified
Otu01068	Proteobacteria	Deltaproteobacteria	Desulfobacterales	Desulfobacteraceae	Desulfobacterium
Otu00744	Spirochaetes	Spirochaetes	Spirochaetales	Leptospiraceae	uncultured_Leptospiraceae
Otu05367	Spirochaetes	Spirochaetes	Spirochaetales	Spirochaetaceae	Spirochaeta
Otu00416	Spirochaetes	Spirochaetes	Spirochaetales	Leptospiraceae	uncultured_Leptospiraceae
Otu01413	Synergistetes	Synergistia	Synergistales	Synergistaceae	Aminobacterium
Otu00713	Verrucomicrobia	Opitutae	Puniceicoccales	Puniceicoccaceae	unclassified
Otu01140	Verrucomicrobia	Verrucomicrobiae	Verrucomicrobiales	Verrucomicrobiaceae	Luteolibacter
Otu01224	Verrucomicrobia	Opitutae	Puniceicoccales	Puniceicoccaceae	marine_group
Otu01477	Verrucomicrobia	OPB35	unclassified	unclassified	unclassified
Otu01660	Verrucomicrobia	Opitutae	Puniceicoccales	Puniceicoccaceae	marine_group
Otu00804	Verrucomicrobia	Opitutae	Puniceicoccales	Puniceicoccaceae	Cerasicoccus

(B) proportion of sequences decreasing with decreasing bottom water oxygen

OTU ID	Phylum	Class	Order	Family	Genus
Otu00293	Acidobacteria	Acidobacteria	Acidobacteriales	Acidobacteriaceae	marine_benthic_group
Otu00630	Acidobacteria	Acidobacteria	Acidobacteriales	Acidobacteriaceae	marine_benthic_group
Otu01965	Acidobacteria	Acidobacteria	Acidobacteriales	Acidobacteriaceae	marine_benthic_group
Otu00648	Acidobacteria	RB25	unclassified	unclassified	Unclassified
Otu00953	Acidobacteria	Holophagae	iii1-8	unclassified	Unclassified
Otu01638	Acidobacteria	RB25	unclassified	unclassified	Unclassified
Otu01653	Acidobacteria	RB25	unclassified	unclassified	Unclassified
Otu05610	Acidobacteria	Acidobacteria	Acidobacteriales	Acidobacteriaceae	uncultured_Acidobacteriaceae
Otu00362	Acidobacteria	Acidobacteria	Acidobacteriales	Acidobacteriaceae	Unclassified
Otu00399	Acidobacteria	RB25	unclassified	unclassified	Unclassified
Otu01677	Acidobacteria	Holophagae	iii1-8	unclassified	Unclassified
Otu02009	Acidobacteria	RB25	unclassified	unclassified	Unclassified
Otu00284	Actinobacteria	Actinobacteria	Acidimicrobidae	Acidimicrobiales	Acidimicrobineae
Otu00319	Actinobacteria	Actinobacteria	Actinobacteridae	Actinomycetales	Streptosporangineae
Otu00301	Actinobacteria	Actinobacteria	Rubrobacteridae	Solirubrobacterales	Conexibacteraceae
Otu00914	Actinobacteria	Actinobacteria	Acidimicrobidae	Acidimicrobiales	Acidimicrobineae
Otu01270	Actinobacteria	Actinobacteria	Acidimicrobidae	Acidimicrobiales	Acidimicrobineae
Otu00483	Actinobacteria	Actinobacteria	Acidimicrobidae	Acidimicrobiales	Acidimicrobineae
Otu01092	Aquificae	Aquificae	Aquificales	Aquificaceae	Hydrogenobaculum
Otu00811	Bacteroidetes	Sphingobacteriia	Sphingobacteriales	WCHB1-69	Unclassified
Otu00710	Bacteroidetes	Sphingobacteriia	Sphingobacteriales	SB-5	Unclassified
Otu01398	Bacteroidetes	Flavobacteriia	Flavobacteriales	Flavobacteriaceae	Unclassified
Otu03654	Bacteroidetes	Flavobacteriia	Flavobacteriales	Flavobacteriaceae	Robiginitalea
Otu00141	Bacteroidetes	Sphingobacteriia	Sphingobacteriales	Flammeovirgaceae	Flexithrix
Otu03701	Candidate_division_OD1	unclassified	unclassified	unclassified	Unclassified
Otu00112	Chloroflexi	Anaerolineae	Anaerolineales	Anaerolineaceae	uncultured_Anaerolineaceae
Otu00030	Chloroflexi	vadinBA26	unclassified	unclassified	Unclassified
Otu00161	Chloroflexi	Anaerolineae	Anaerolineales	Anaerolineaceae	uncultured_Anaerolineaceae
Otu00363	Chloroflexi	Anaerolineae	Anaerolineales	Anaerolineaceae	uncultured_Anaerolineaceae
Otu00435	Chloroflexi	Caldilineae	Caldilineales	Caldilineaceae	Caldilinea
Otu00463	Chloroflexi	Anaerolineae	Anaerolineales	Anaerolineaceae	uncultured_Anaerolineaceae
Otu00485	Chloroflexi	Anaerolineae	Anaerolineales	Anaerolineaceae	uncultured_Anaerolineaceae
Otu00490	Chloroflexi	Anaerolineae	Anaerolineales	Anaerolineaceae	uncultured_Anaerolineaceae
Otu01080	Chloroflexi	Anaerolineae	Anaerolineales	Anaerolineaceae	uncultured_Anaerolineaceae
Otu01408	Chloroflexi	Anaerolineae	Anaerolineales	Anaerolineaceae	uncultured_Anaerolineaceae
Otu03033	Chloroflexi	Anaerolineae	Anaerolineales	Anaerolineaceae	uncultured_Anaerolineaceae
Otu03249	Chloroflexi	Caldilineae	Caldilineales	Caldilineaceae	uncultured_Caldilineaceae
Otu00026	Chloroflexi	Caldilineae	Caldilineales	Caldilineaceae	uncultured_Caldilineaceae
Otu00356	Chloroflexi	unclassified	unclassified	unclassified	Unclassified
Otu00832	Chloroflexi	Caldilineae	Caldilineales	Caldilineaceae	uncultured_Caldilineaceae
Otu00987	Chloroflexi	Anaerolineae	Anaerolineales	Anaerolineaceae	uncultured_Anaerolineaceae
Otu05804	Cyanobacteria	SubsectionIII	Halomicronema	unclassified	Unclassified
Otu03667	Deferribacteres	Unclassified_Deferribacterales	LCP-89	unclassified	Unclassified
Otu01063	Deinococcus-Thermus	Thermales	Thermaceae	Marinithermus	Unclassified
Otu01296	Firmicutes	Clostridia	Clostridiales	Heliobacteriaceae	Heliorestis
Otu00314	Firmicutes	Clostridia	Clostridiales	JTB215	unclassified
Otu00320	Firmicutes	Clostridia	Clostridiales	JTB215	unclassified
Otu00958	Firmicutes	Clostridia	Thermoanerobacteral	Thermoanaerobacteraceae	Thermoanaerobacteraceae

			es		
Otu01293	Firmicutes	Clostridia	Clostridiales	Veillonellaceae	Schwartzia
Otu01975	Firmicutes	Clostridia	Thermoanerobacterales	Thermoanaerobacteraceae	Thermoanaerobacteraceae
Otu00267	Firmicutes	Clostridia	Clostridiales	Veillonellaceae	Schwartzia
Otu00274	Firmicutes	Clostridia	Clostridiales	Ruminococcaceae	Uncultured_Ruminococcaceae
Otu00233	Gemmatimonadetes	Gemmatimonadetes	PAUC43f_marine_benthic_group	unclassified	unclassified
Otu00524	Hyd24-12	unclassified	unclassified	unclassified	unclassified
Otu00544	Planctomycetes	Phycisphaerae	vadinBA30	unclassified	unclassified
Otu02533	Planctomycetes	Phycisphaerae	SHA-43	unclassified	unclassified
Otu00295	Proteobacteria	Deltaproteobacteria	Sh765B-TzT-29	unclassified	unclassified
Otu00650	Proteobacteria	Alphaproteobacteria	Sphingomonadales	Sphingomonadaceae	unclassified
Otu00778	Proteobacteria	Gammaproteobacteria	KI89A_clade	unclassified	unclassified
Otu00782	Proteobacteria	Deltaproteobacteria	Desulfobacterales	Nitrospinaceae	Uncultured_Nitrospinaceae
Otu00908	Proteobacteria	Gammaproteobacteria	Xanthomonadales	JTB255_marine_benthic_group	unclassified
Otu00970	Proteobacteria	Deltaproteobacteria	Desulfobacterales	Nitrospinaceae	Uncultured_Nitrospinaceae
Otu00974	Proteobacteria	Gammaproteobacteria	JTB148	unclassified	unclassified
Otu00991	Proteobacteria	Gammaproteobacteria	unclassified	unclassified	unclassified
Otu02167	Proteobacteria	Alphaproteobacteria	Rhodobacterales	Rhodobacteraceae	unclassified
Otu00181	Proteobacteria	Alphaproteobacteria	Rhizobiales	unclassified	unclassified
Otu00414	Proteobacteria	Gammaproteobacteria	Legionellales	Legionellaceae	Uncultured
Otu00616	Proteobacteria	Deltaproteobacteria	Desulfobacterales	Desulfobacteraceae	Desulforegula
Otu01122	Proteobacteria	Deltaproteobacteria	Sh765B-TzT-29	unclassified	unclassified
Otu01171	Proteobacteria	Gammaproteobacteria	Xanthomonadales	JTB255_marine_benthic_group	unclassified
Otu01245	Proteobacteria	Deltaproteobacteria	Myxococcales	Nannocystineae	uncultured
Otu01367	Proteobacteria	Gammaproteobacteria	Xanthomonadales	JTB255_marine_benthic_group	unclassified
Otu01567	Proteobacteria	Deltaproteobacteria	Myxococcales	Nannocystineae	uncultured
Otu01572	Proteobacteria	Deltaproteobacteria	Myxococcales	Sorangiineae	Phaselicystidaceae
Otu02647	Proteobacteria	Deltaproteobacteria	Sh765B-TzT-29	unclassified	unclassified
Otu03915	Proteobacteria	Deltaproteobacteria	Desulfobacterales	Desulfobacteraceae	uncultured_Desulfobacteraceae
Otu00003	Proteobacteria	Deltaproteobacteria	Syntrophobacterales	Syntrophobacteraceae	uncultured_Syntrophobacteraceae
Otu00032	Proteobacteria	Deltaproteobacteria	Myxococcales	JG37-AG-15	unclassified
Otu00137	Proteobacteria	Gammaproteobacteria	Legionellales	Legionellaceae	uncultured_Legionellaceae
Otu00162	Proteobacteria	Deltaproteobacteria	Sva0485	unclassified	unclassified

table S5. Ranking of most abundant bacterial OTUs (without singletons) in decreasing order of their relative sequence abundance (in %) across all samples.

OTU	Genus	Family	Order	Class	Phylum	Total (%)	oxic			oxic/ hypoxic	anoxic/ hypoxic	anoxic		
							462 (0-1)	462 (4-5)	462 (9-10)	487 (0-1)	393 (0-1)	448 (0-1)	448 (4-5)	448 (9-10)
Otu00001	Lutimonas	Flavobacteriaceae	Flavobacteriales	Flavobacteriia	Bacteroidetes	5.4	2.0	0.3	0.0	0.6	0.6	1.5	0.3	0.1
Otu00002	unclassified	Syntrophobacteraceae	Syntrophobacterales	Deltaproteobacteria	Proteobacteria	2.8	0.5	0.2	0.1	0.2	0.8	0.3	0.5	0.2
Otu00003	Desulfobulbus	Desulfobulbaceae	Desulfobacterales	Deltaproteobacteria	Proteobacteria	2.7	0.2	1.0	1.2	0.0	0.2	0.0	0.0	0.1
Otu00004	Lutibacter	Flavobacteriaceae	Flavobacteriales	Flavobacteriia	Bacteroidetes	2.0	0.2	0.3	0.0	0.5	0.5	0.1	0.3	0.1
Otu00005	unclassified	Desulfobacteraceae	Desulfobacterales	Deltaproteobacteria	Proteobacteria	1.8	0.0	0.0	0.0	0.6	0.9	0.2	0.1	0.0
Otu00008	Robiginitalea	Flavobacteriaceae	Flavobacteriales	Flavobacteriia	Bacteroidetes	1.7	0.2	0.4	0.0	0.1	0.6	0.0	0.2	0.2
Otu00006	unclassified	JTB255 marine benthic group	Xanthomonadales	Gammaproteobacteria	Proteobacteria	1.7	0.1	0.0	0.0	0.2	0.7	0.4	0.1	0.1
Otu00011	Desulfobacula	Desulfobacteraceae	Desulfobacterales	Deltaproteobacteria	Proteobacteria	1.2	0.1	0.0	0.0	0.5	0.3	0.1	0.2	0.0
Otu00012	Lutibacter	Flavobacteriaceae	Flavobacteriales	Flavobacteriia	Bacteroidetes	1.1	0.0	0.0	0.0	0.4	0.0	0.6	0.1	0.0
Otu00009	unclassified	Caldilineaceae	Caldilineales	Caldilineae	Chloroflexi	1.1	0.0	0.0	0.0	0.3	0.3	0.3	0.1	0.0
Otu00013	unclassified	Anaerolineaceae	Anaerolineales	Anaerolineae	Chloroflexi	0.9	0.3	0.1	0.2	0.0	0.1	0.0	0.0	0.0
Otu00018	unclassified	Desulfobacteraceae	Desulfobacterales	Deltaproteobacteria	Proteobacteria	0.8	0.0	0.1	0.2	0.0	0.2	0.1	0.1	0.1
Otu00019	Lutibacter	Flavobacteriaceae	Flavobacteriales	Flavobacteriia	Bacteroidetes	0.8	0.0	0.2	0.3	0.0	0.1	0.0	0.0	0.1
Otu00033	unclassified	Caldilineaceae	Caldilineales	Caldilineae	Chloroflexi	0.8	0.1	0.0	0.0	0.1	0.0	0.2	0.3	0.0
Otu00026	unclassified	Flavobacteriaceae	Flavobacteriales	Flavobacteriia	Bacteroidetes	0.7	0.3	0.1	0.2	0.0	0.1	0.0	0.0	0.1
Otu00015	unclassified	Desulfobacteraceae	Desulfobacterales	Deltaproteobacteria	Proteobacteria	0.7	0.1	0.0	0.0	0.3	0.1	0.2	0.1	0.0
Otu00036	unclassified	Desulfobacteraceae	Desulfobacterales	Deltaproteobacteria	Proteobacteria	0.7	0.0	0.1	0.1	0.1	0.3	0.0	0.1	0.0
Otu00020	Desulfococcus	Desulfobacteraceae	Desulfobacterales	Deltaproteobacteria	Proteobacteria	0.7	0.0	0.1	0.1	0.0	0.3	0.0	0.1	0.1
Otu00038	unclassified	Sva1033	Desulfuromonadales	Deltaproteobacteria	Proteobacteria	0.7	0.0	0.0	0.0	0.1	0.1	0.1	0.2	0.1

table S6. Contribution (%) of each hypothesized relationship (path) to global explained variability [global R^2; see Tenenhaus *et al.* (*108*) for details]. The goodness-of-fit (GoF) index of the path model was 0.75. **P*<0.05; ***P* <0.01; ****P* < 0.001, ° marginally significant trend with *P* = 0.08.

Path coefficient	Path interpretation	Correlation	Contribution to global R^2 (%)
0.77***	Increasing bottom water oxygen increases bioturbation	0.77	12
-0.43°	Increasing bottom water oxygen decreases organic matter concentration	-0.8	7
0.83***	Increasing bottom water oxygen increases faunal diversity	0.83	14
0.88***	Increasing bottom water oxygen increases faunal respiration	0.88	16
0.95***	Increasing bottom water oxygen increases aerobic microbial respiration	0.96	19
-0.75**	Increasing bottom water oxygen decreases anaerobic microbial respiration	-0.75	12
-0.49*	Increasing bioturbation decreases organic matter concentration	-0.82	8
-0.83**	Increasing bioturbation decreases bacterial diversity	-0.73	12

table S7. Abundance of macrofauna and meiofauna taxa of the northwestern Crimean Shelf. Macrofaunal (A) and meiofaunal (B) composition and abundance data used for Figure S7 (x 10^3 and x10^4 individuals m^{-2} respectively) per station at the outer Western Crimean Shelf. Results are integrated over the upper 5 cm. Data from Lichtschlag et al., (*37*).

(A) Macrofauna

Station	Bivalvia	Cnidaria	Gastropoda	Oligochaeta	Polychaeta
462	0.4	0.4	0.4	0.3	0.8
459	0	50.1	0	0.6	0.1
487	0	23.4	0	2.6	0.3
513	0	1.7	0	0.7	0
393	0	0	0	0.1	0
506	0	0	0	0	0
448	0	0	0	0	0

(B) Meiofauna

Station	Acari	Bivalvia	Ciliophora	Cnidaria	Forams_hard	Forams_soft	Gastropoda	Gromia	Harpacticoida	Kinorhyncha	Nauplia_Decapoda	Nematoda	Nemertini	Oligochaeta_juvenile	Ostracoda	Polychaeta	Tardigrada	Turbellaria
462	0.26	0.2	0.16	0.03	0.09	0.37	0.03	0.66	1.3	0.12	0.26	128.75	0.01	0.32	2.8	0.66	0.57	1.38
459	0.01	0.16	1.52	1.14	0.16	3.56	0.01	3.32	0.76	0.32	0	183.06	0	0.01	0	0.58	0	4.33
487	0	0.23	3.55	3.8	15.42	7.68	0.01	2.28	3.46	0.01	0.43	134.44	0.01	0.04	0.01	0.42	0	0.33
513	0	0.88	3.49	0.98	2.49	17.88	0	0.6	0.14	0	0	82.78	0	0	0	0.22	0	0.02
393	0	0.06	0.97	0.04	0.01	0.19	0	0	0.19	0	0	3.36	0	0	0	0.18	0	0
506	0	0	0	0	0	0	0	0	0	0	0	0	0	0	0	0	0	0
448	0	0	0	0	0	0	0	0	0	0	0	0	0	0	0	0	0	0

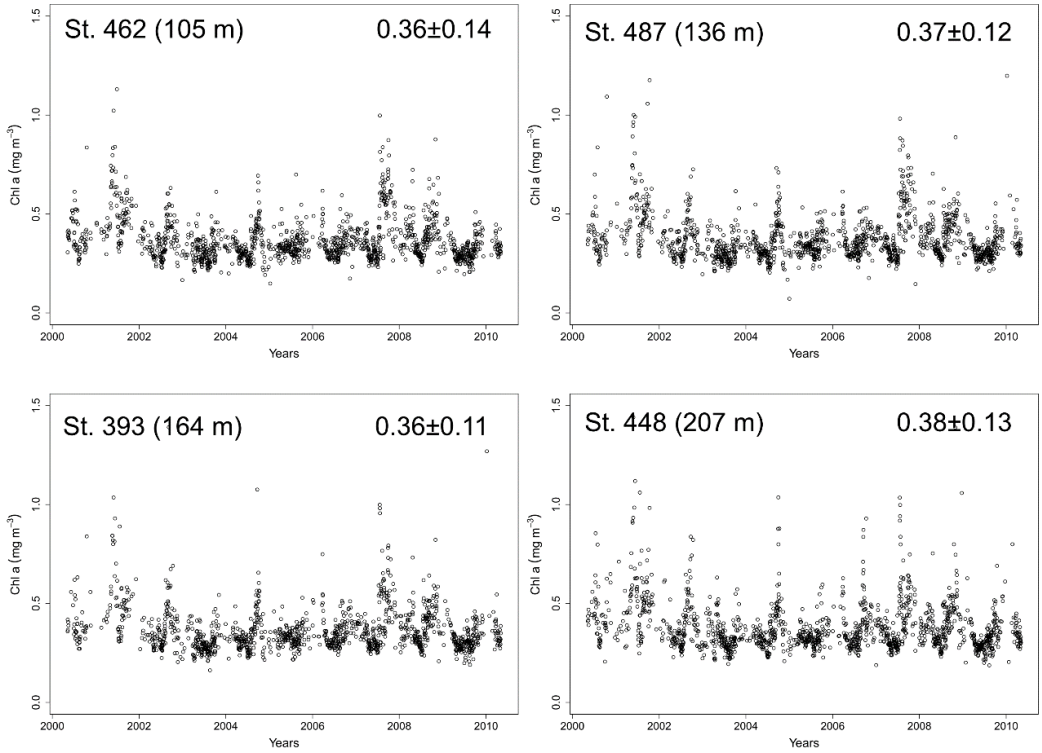

fig. S1. Ten years (5 May 2000 to 5 May 2010) of satellite-based surface chlorophyll a concentration. Satellite data variation in chlorophyll *a* content of surface waters fluctuated both spatially and temporally only within a concentration of ±0.1 mg m^{-3}, indicating relatively similar rates of productivity and particle flux within the study area. Data generated using *MyOcean* Products (Marine Copernicus, 2015), results from the merging of SeaWiFS, MODIS-Aqua and MERIS sensors. Values represent average and standard deviation (±).

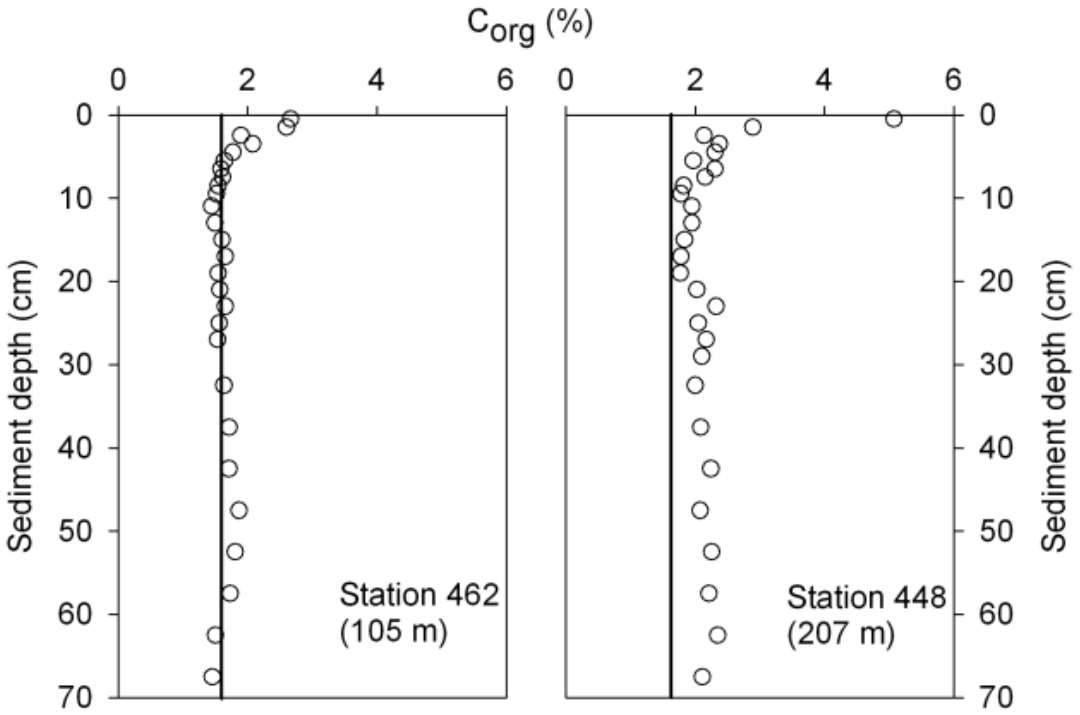

fig. S2. Downcore organic carbon (%C_{org}) in the upper 70 cm comparing permanent oxic (station 462, 105 m) and anoxic (station 448, 207 m) conditions on the Crimean shelf. The vertical line at ~1.6% Corg depicts the lowest Corg contents in samples obtained, assumed to be the threshold for remineralization in the time frame of 40 years (based on ^{210}Pb; (*37*)).

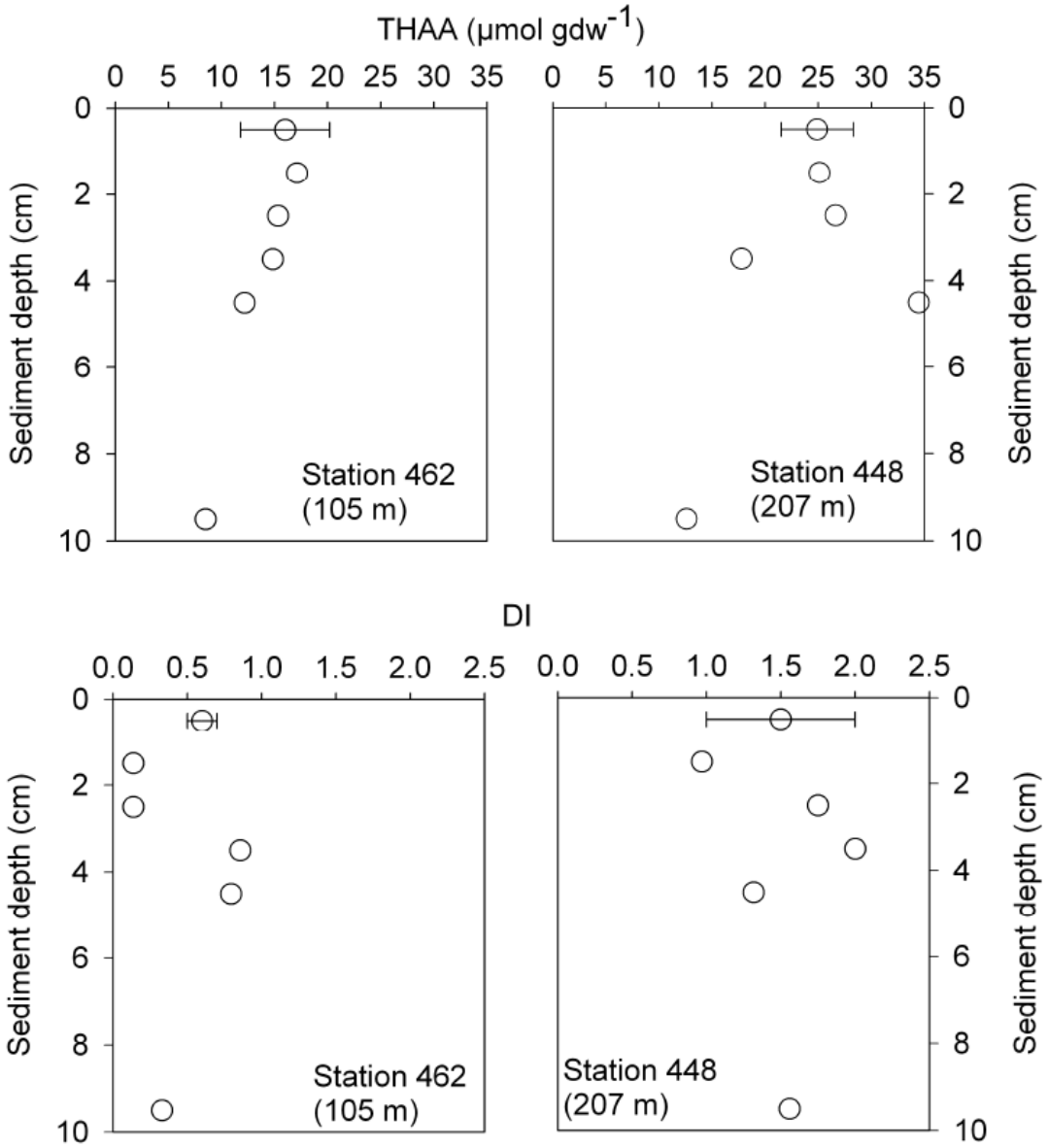

fig. S3. Downcore THAA concentrations (µmol gdw^{-1}) and DI comparing permanent oxic (station 462, 105 m) and anoxic (station 448, 207 m) conditions on the Crimean shelf.

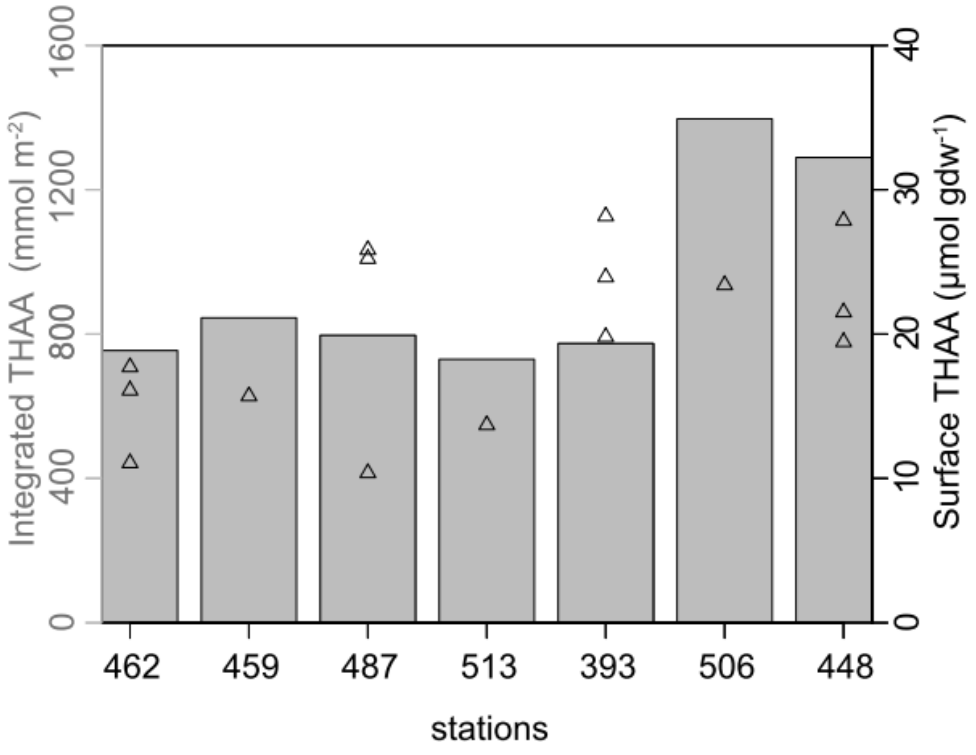

fig. S4. THAA concentration integrated 0 to 5 cm (bars) and THAA surface concentrations (triangles).

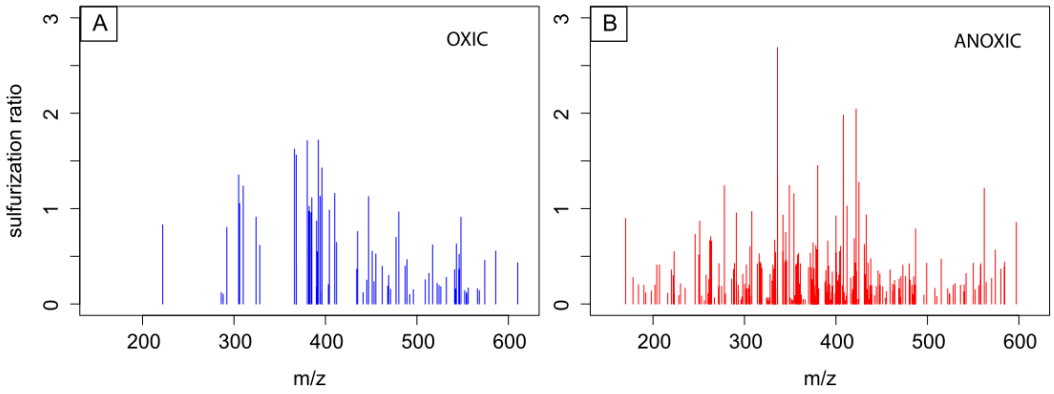

fig. S5. (**A** and **B**) Sulfurization ratio for molecular formulae unique for oxic and anoxic conditions respectively (0-10 cm).

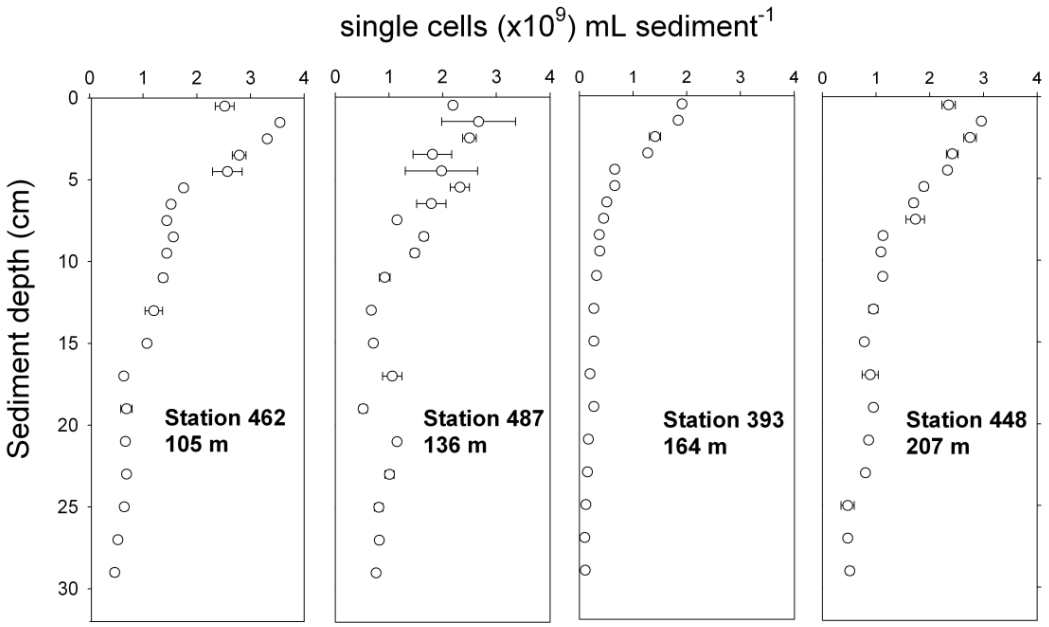

fig. S6. Downcore cell abundances [single cells ($\times 10^9$) ml sediment^{-1}], in the upper 30 cm, comparing oxygen regimes on the Crimean shelf. Values represent average and standard deviation of counting (30 grids, 2 filters).

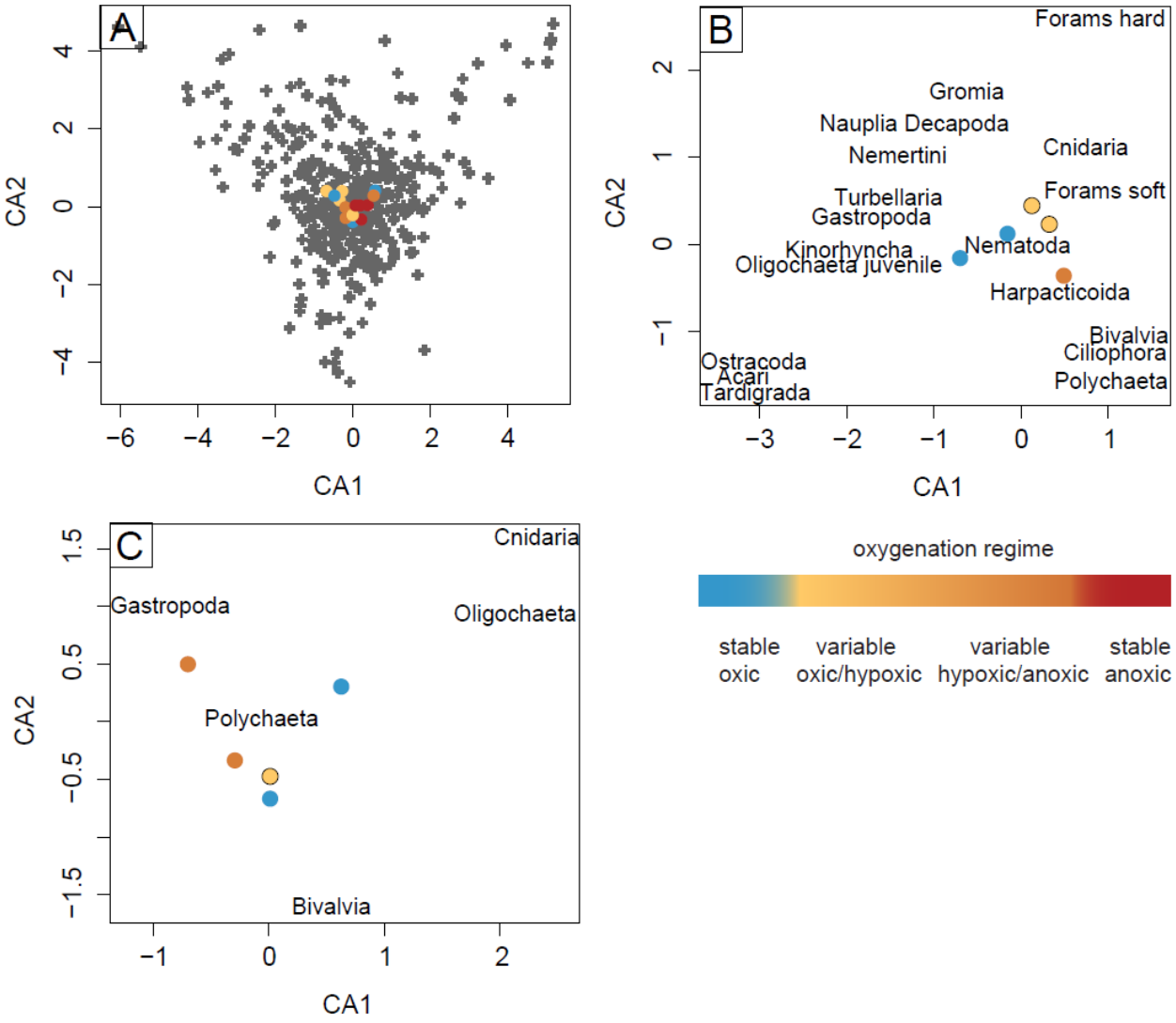

fig. S7. Ordination biplots generated by Correspondence Analysis (CA) of (**A**) bacterial communities (based on ARISA fingerprinting), (**B**) meiofaunal and (**C**) macrofaunal abundances of each taxonomic group. Circles represent different oxygen regimes according to color code, grey crosses in panel A represent OTUs of ARISA profiles.

107. M. Tenenhaus, V. E. Vinzi, Y.-M. Chatelin, C. Lauro, PLS path modeling. *Comput. Stat. Data Anal.* **48**, 159–205 (2005).

Acknowledgments: We thank the officers, crew, and shipboard scientific party of *RV Maria S. Merian* for support at sea during the MSM 15-1 expedition. We would also like to thank F. Janssen, A. Nordhausen, D. Donis, W. Stiens, R. Stiens, M. Alisch, E. Weiz-Bersch, and M. Meiners for their assistance on board and in the laboratory; P. L. Buttigieg for helpful discussions; L. Núñez and P. Concha for their help with amino acid analysis; and J. Cartes for help with the conceptual diagram. We thank J. Niggemann and T. Dittmar for support with DOM analyses. We also thank two anonymous reviewers for their helpful comments and suggestions. **Funding:** This study was financially supported by the European Union's Seventh Framework Programme project HYPOX "In situ monitoring of oxygen depletion in hypoxic ecosystems of coastal and open seas, and land-locked water bodies" (European Council grant 226213), the European Research Council AdvG Abyss (294757) to A.B., and COPAS Sur-Austral (CONICYT PIA PFB31) to S.P. **Author contributions:** A.B. initiated and planned the study. G.L.J., A.L., and A.B. conducted the field campaign. G.L.J. performed microbiological analyses. C.J.S., U.S., S.P., P.E.R., and G.L.J. performed chemical analyses. G.L.J. and A.R. carried out bioinformatics and statistical analyses. All authors contributed to data analysis and the writing of the paper. **Competing interests:** The authors declare that they have no competing interests. **Data and materials availability:** All data needed to evaluate the conclusions in the paper are present in the paper and/or the Supplementary Materials. Additional data related to this paper may be requested from the authors. All data are available online in the Data Publisher for Earth and Environmental Science (PANGAEA).

Submitted 11 August 2016
Accepted 4 January 2017
Published 10 February 2017
10.1126/sciadv.1601897

Citation: G. L. Jessen, A. Lichtschlag, A. Ramette, S. Pantoja, P. E. Rossel, C. J. Schubert, U. Struck, A. Boetius, Hypoxia causes preservation of labile organic matter and changes seafloor microbial community composition (Black Sea). *Sci. Adv.* **3**, e1601897 (2017).

Hypoxia causes preservation of labile organic matter and changes seafloor microbial community composition (Black Sea)

Gerdhard L. Jessen, Anna Lichtschlag, Alban Ramette, Silvio Pantoja, Pamela E. Rossel, Carsten J. Schubert, Ulrich Struck and Antje Boetius (February 10, 2017)

Sci Adv 2017, 3:.
doi: 10.1126/sciadv.1601897